Differential Effects of α Subunit Asparagine 56 Oligosaccharide Structure on Equine Lutropin and Follitropin Hybrid Conformation and Receptor−Binding Activity †

ARTICLE *in* BIOCHEMISTRY · SEPTEMBER 2004

Impact Factor: 3.02 · DOI: 10.1021/bi049857p · Source: PubMed

Differential Effects of α Subunit Asparagine[56] Oligosaccharide Structure on Equine Lutropin and Follitropin Hybrid Conformation and Receptor-Binding Activity[†]

George R. Bousfield,*[,‡] Vladimir Y. Butnev,[‡] Viktor Y. Butnev,[‡] Van T. Nguyen,[‡] Ciann M. Gray,[‡] James A. Dias,[§] Robert MacColl,[§] Leslie Eisele,[§] and David J. Harvey[||]

Department of Biological Sciences, Wichita State University, Wichita, Kansas 67260, Wadsworth Institute, State of New York Health Department, Albany, New York 12201, and Glycobiology Institute, Department of Biochemistry, Oxford University, Oxford, OX1 2JD United Kingdom

Received January 19, 2004; Revised Manuscript Received May 14, 2004

ABSTRACT: The gonadotropins, luteinizing hormone (LH), follicle-stimulating hormone (FSH), and chorionic gonadotropin (CG), are cysteine-knot growth-factor superfamily glycoproteins composed of a common α subunit noncovalently associated with a hormone-specific *β* subunit. The cysteine-knot motifs in both subunits create two hairpin loops, designated L1 and L3, on one side of the knot, with the intervening long loop, L2, on the opposite side. As the average α-subunit loop 2 oligosaccharide mass increased from 1482 to 2327, LH and FSH receptor-binding affinities of the dual-specificity eLH declined significantly, while the decrease in FSH receptor-binding affinity for eFSH was not significant. In the present study, we characterized hormone-specific glycosylation of αL2 oligosaccharides in eLHα, eFSHα, and eCGα preparations. MALDI mass spectrometry revealed 28−57 structures, including high mannose, hybrid, bi-, and triantennary oligosaccharides. The same intact subunit preparations and their αL2 loop-deglycosylated derivatives were combined with either eLH*β* or eFSH*β*, and the circular dichroism (CD) spectrum for each preparation was determined. We predicted that hybrid hormone preparations obtained by combining intact eLHα, eFSHα, and eCGα preparations with eLH*β* might exhibit differences in conformation that would disappear when the αL2 oligosaccharide attached to αAsn[56] was removed by selective peptide-*N*-glycanase digestion (N[56]dg-α). CD data supported the first prediction; however, elimination of αL2 oligosaccharide actually increased the conformational differences. The intact α subunit: eFSH*β* hybrids had virtually identical CD spectra, as expected. However, the N[56]dg-α:eFSH*β* hybrid spectra differed from each other. Oligosaccharide removal altered the conformation of most hybrids, suggesting that αAsn[82] oligosaccharide (located in αL3) also influenced gonadotropin conformation.

The glycoprotein hormones, lutropin (LH),[1] follitropin (FSH), thyrotropin (TSH), and choriogonadotropin (CG), represent the most complex family of classical trophic hormones (*1*). Each member of this unusual family in the cysteine-knot growth-factor superfamily is composed of a common α subunit noncovalently embraced by a hormone-specific *β* subunit. While only the heterodimers bind their cognate receptors at physiological concentrations, heterodimer formation is not sufficient for receptor binding. Subunit reassociation studies with hCG and hFSH revealed rapidly formed, transient, nonfunctional heterodimeric intermediates that could not bind their cognate receptors (*2*, *3*). The rate-limiting step for hormone reconstitution from subunits involved these intermediates slowly transforming into receptor-binding-competent hormones, presumably undergoing conformational change(s) in the process.

LH and FSH bind heptahelical G protein-coupled receptors that each possess an unusually large amino-terminal extracellular domain, which provides the high-affinity binding site (*4*). The transmembrane domain of the LH receptor appears to possess a low-affinity binding site (*5*). While gonadotropin receptor binding is necessary, it is not sufficient for target-cell activation, because the gonadotropin carbohydrate moieties participate in this process by an unknown mechanism. Both glycoprotein hormone α and *β* subunits are glycosylated, and their carbohydrate moieties appear to contribute to cellular activation in a nonequivalent manner.

[†] Hormone preparations employed in this study were derived from work supported by NIH Grant AG15428. Mass spectrometry was supported by NIH Grant RR-16475 from the BRIN Program of the National Center for Research Resources and the Biotechnology and Biological Sciences Research Council.

* To whom correspondence should be addressed: Department of Biological Sciences, Wichita State University, 1845 Fairmount, Wichita, KS 67260-0026. Phone: 316-978-6088. Fax: 316-978-3772. E-mail: george.bousfield@wichita.edu.

[‡] Wichita State University.

[§] State of New York Health Department.

[||] Oxford University.

[1] Abbreviations: LH, luteinizing hormone; FSH, follicle-stimulating hormone; TSH, thyroid-stimulating hormone; CG, chorionic gonadotropin; BSA, bovine serum albumin; CD, circular dichroism; DHB, 2,5-dihydoxybenzoic acid; Gal, galactose; GlcNAc, *N*-acetylglucosamine; GuHCl, guanidine hydrochloride; HPLC, high-performance liquid chromatography; MALDI, matrix-assisted laser desorption ionization; Man, mannose; Neu5Ac, *N*-acetylneuraminic acid; Neu5Gc, *N*-glycoylneuraminic acid; Neu4,5Ac$_2$, *N*,*O*-diacetylneuraminic acid; PNGase-F, peptide *N*-glycosidase F; RLA, radioligand assay; SDS, sodium dodecyl sulfate; TFA, trifluoroacetic acid. Species designations for gonadotropins are indicated by a lowercase letter preceding the hormone abbreviation: e, equine (horse); h, human; and o, ovine. The common α subunit and hormone-specific *β* subunits are indicated with corresponding Greek characters.

10.1021/bi049857p CCC: $27.50
Published on Web 07/29/2004

The α subunits are invariantly glycosylated at two sites, Asn^{56} (Asn^{52} in humans) in the long loop, αL2, and Asn^{82} (Asn^{78} in humans) in αL3. The *β* subunits are variably glycosylated at one or two highly conserved positions, Asn^{13} and Asn^{30} in hCG*β*, Asn^{13} in most mammalian LH*β* subunits (Asn^{30} in hLH*β*), at the Asn^{30}-homologous position, Asn^{23}, in TSH*β*, and at both homologous positions in FSH*β*, Asn^{7} and Asn^{24}. All *β*-subunit N-glycosylation sites are located in the *β*L1 loop. The α-subunit oligosaccharides attached to Asn^{52} or Asn^{56} play a primary role in signal transduction initiated by the LH and FSH receptors (*6*−*8*). A secondary signaling role for *β*Asn^{13} oligosaccharides was reported for both oLH and hCG (*6*, *9*). Studies involving the latter demonstrated that prior elimination of αAsn^{52} oligosaccharide was necessary before a functional role for *β*Asn^{13} carbohydrate was detectable (*6*). The structures of Asn^{56} oligosaccharides vary in a hormone-specific manner (*10*). Indeed, the oligosaccharide profile obtained by high pH anion-exchange chromatography could reveal the identity of the hormone from which it was derived. As the average αAsn^{56} oligosaccharide mass increased from 1482 to 2327, LH and FSH receptor-binding affinities of eLH hybrids, which bound both LH and FSH receptors, declined significantly (*11*). The binding of eLH to the FSH receptor was affected to an even greater extent by increased oligosaccharide size than the binding to its cognate receptor. However, although eFSH hybrid binding to the FSH receptor declined as average Asn^{56} oligosaccharide mass increased, the magnitude of the differences was reduced to the point that the decrease was not statistically significant (*11*, *12*). Two hypotheses have been proposed to explain the greater impact of Asn^{56} oligosaccharide structure on LH binding its receptor than FSH binding the FSH receptor. The first was that Asn^{56} carbohydrate inhibited receptor binding by steric hindrance on the part of a complex carbohydrate branch attaching *β*(1−4) to the α(1−6)Man residue of the pentasaccharide core. Because FSH and LH/CG were assumed to bind their respective receptors in a different orientation, steric hindrance on the part of αAsn^{56} oligosaccharides was relatively low for FSH and relatively high for LH/CG (*11*). Extensive structural characterization was undertaken to confirm that the complex oligosaccharide branch was indeed absent in eLHα oligosaccharides, present in eFSHα oligosaccharides, and extended by a lactosamine repeat in eCGα. The second hypothesis, that the oligosaccharide structural differences had less of an effect on FSH conformation than on LH/CG conformation, was tested using circular dichrosim (CD).

In the present study, we confirmed that αAsn^{56} oligosaccharides inhibited binding to the LH receptor itself, better defined these oligosaccharide structures using mass spectrometry, and observed differential effects of oligosaccharide on the secondary structure that implicated Asn^{82} glycosylation. Equine LH*β* hybrid conformation differed, while the same αAsn^{56} oligosaccharides did not affect eFSH*β* hybrid conformation to an appreciable extent. In fact, although different families of oligosaccharides resided at this position, their presence seemed to stabilize a single conformation, as indicated by the similarities in the CD spectra obtained for intact eFSH hybrids, while their absence permitted the conformation to vary, depending on the Asn^{56}-deglycosylated α subunit associated with eFSH*β*, possibly as a consequence of differences in αAsn^{82} oligosaccharide structures.

EXPERIMENTAL PROCEDURES

Hormone Preparations. Equine gonadotropins, eLH, eFSH, eCG, and their respective α and *β* subunits were prepared as described previously (*11*, *13*, *14*). Selective αAsn^{56} deglycosylation of α subunits using PNGase-F (EC 3.5.1.52) followed a previously published procedure (*10*). Association of intact and Asn^{56}-deglycosylated α subunit with either eLH*β* and eFSH*β* to create a series of eLH and eFSH hybrids proceeded as described before (*11*), except that separation of eFSH hybrids from unassociated subunits was accomplished by gel filtration using a 2.5 × 200 cm Sephacryl S-200 column (*15*).

Radioligand Assay. An institutional animal care and use committee approved all animal procedures. Receptor-binding assays were performed using 25 mg rat testis homogenate tissue/tube and 2.5 ng of either ^{125}I-eFSH or ^{125}I-hCG tracer. The chloramine T technique was used for iodination, producing specific activities of 30−50 *μ*Ci/*μ*g. Duplicate assay tubes were incubated for 2 h at 37 °C in a shaking water bath and were then centrifuged. The supernatant was aspirated, and the pellet was counted in a Packard (Meriden, CT) Cobra II *γ* counter. The counting efficiency was >74%. The eLH*β* hybrids were tested in both LH and FSH assays, while eFSH*β* hybrids were tested in only the LH assay, because they exhibit very low LH receptor-binding activity (*16*).

Solubilized LH receptors were prepared from rat testis homogenate, which was obtained following Dounce homogenization in 0.1 M Tris-HCl at pH 7.5, containing 0.02% sodium azide and 0.1% BSA (RLA buffer). The homogenate was centrifuged at 2000*g* for 20 min at 4 °C. The supernatant was discarded, and the pellet was solubilized with 0.1% Triton X-100 in RLA buffer containing 30% glycerol, by slow shaking at 4 °C for 1.5 h, followed by centrifugation at 50000*g* for 1 h at 4 °C. Buffer or cold hormone and ^{125}I-hCG tracer were combined with 50 mg equivalent solubilized rat testis homogenate in a total volume of 400 *μ*L and incubated overnight at 4 °C. After incubation, 0.1 mL of decomplemented calf serum, 0.3 mL of RLA buffer with 20% glycerol, and 1 mL of 20% poly(ethylene glycol) solution in RLA buffer, containing 20% glycerol, were added to each tube. The tubes were vortexed for 30 s each and centrifuged at 2620*g* for 20 min at 4 °C. The supernatants were removed by aspiration, and the ^{125}I bound to the pellet counted in the *γ* counter.

MALDI−*MS of αAsn^{56} Oligosaccharides.* Oligosaccharides recovered from eLHα, eFSHα, and eCGα by PNGase-F digestion, followed by Amicon Centricon P-10 (Millipore, Billerica, MA) ultrafiltration were adsorbed to 150 mg Alltech (Deerfield, IL) Carbograph cartridges previously washed with 3 mL of 80% acetonitrile/0.1% TFA/water followed by 3 mL of Milli-Q water. After sample application, the cartridges were washed with 3 mL of water and oligosaccharides were eluted with 3 mL of 25% acetonitrile/water containing 0.025% TFA (*17*). Oligosaccharides were recovered by evaporation using a Thermo Savant (Holbrook, NY) SpeedVac. Carbohydrate recovery was determined by monosaccharide analysis of samples hydrolyzed for 4 h at 100 °C in 4 N TFA using a Dionex (Sunnyvale, CA) carbohydrate analyzer (*18*). Preparative fractionation of 350 nmol samples of eLHα Asn^{56} oligosaccharides by high pH

anion-exchange chromatography employed a 0.9 × 25 cm Dionex PA-1 column at a flow rate of 5 mL/min, as previously reported (*18*). Chromatographic fractions were immediately desalted using Carbograph cartridges, as described above.

Oligosaccharide samples (1 μL) were desalted with a Nafion-117 membrane according to the procedure described by Börnsen et al. (*19*). MALDI−MS was carried out using a Waters-Micromass (Manchester, UK) TofSpec 2E reflectron time-of-flight mass spectrometer fitted with a N_2 (337 nm, 3 ns pulse) laser and a delayed extraction ion source. Samples were prepared by mixing an aqueous solution (0.3 μL) of the glycans with the MALDI matrix [0.3 μL of a saturated solution of 2,5-dihydroxybenzoic acid (DHB) in acetonitrile] on the MALDI target plate, allowing the mixture to dry under ambient conditions, and recrystallizing the mixture from ethanol. Positive ion mass spectra were acquired in reflectron mode with an acceleration voltage of 20 kV. Negative ion spectra were acquired with the same instrument under similar conditions.

MS/MS. Most of the MS/MS data were acquired with a Micromass hybrid quadrupole-time-of-flight (Q-TOF) mass spectrometer fitted with a nanospray ion source, and a few samples were also examined with a similar instrument equipped with a MALDI ion source (*20*). For the electrospray experiments, samples were dissolved in a mixture of water and methanol (1:1 by volume) and infused with Micromass borosilicate capillaries type F. The capillary voltage was varied between 2 and 3 kV, and the cone voltage was set to 200 V to produce $[M + Na]^+$ ions (*20*). Ions were selected for fragmentation with a 2−3 Da window and fragmented in the collision cell with argon as the collision gas. The collision cell voltage was adjusted for each compound to produce an even distribution of ions over the mass range. MALDI−MS/MS spectra were acquired from DHB under similar conditions with the targets prepared as described above.

Exoglycosidase Sequencing. All exoglycosidases were purchased from Glyko, Inc. (Novato, CA). Glycans were digested in a volume of 10 μL for 18 h at 37 °C in 50 mM sodium acetate buffer at pH 5.5, using arrays of the following enzymes: *Arthrobacter ureafaciens* sialidase (EC 3.2.1.18), 1 unit/mL; Newcastle disease virus neuraminidase (EC 3.2.1.18), 200 milliunits/mL; almond meal α-fucosidase (EC 3.2.1.111), 3 milliunits/mL; bovine kidney fucosidase (EC 3.2.1.51), 1 unit/mL; *Streptococcus pneumoniae* galactosidase (EC 3.2.1.23), 0.1 unit/mL; bovine testes β-galactosidase (EC 3.2.1.23), 1 unit/mL; *Streptococcus pneumoniae β-N*-acetylhexosaminidase (EC 3.2.1.30), 120 milliunits/mL; Jack bean *β-N*-acetylhexosaminidase (EC 3.2.1.30), 10 milliunits/mL; and Jack bean α-mannosidase (EC 3.2.1.24), 50 units/mL. After incubation, enzymes were removed by filtration through a protein-binding nitrocellulose membrane (Pro-Spin 45 μm CN filters, Radley and Co., Ltd., Essex, U.K.) and oligosaccharides were analyzed by MALDI−MS.

CD of Hybrids. Hybrid hormone preparations were weighed and dissolved in 0.01 M sodium phosphate buffer and 0.15 M NaCl at pH 7. Protein concentrations were determined by amino acid analysis performed on 100−200 μL aliquots. CD measurements employed a Jasco (Japan Spectroscopic Co., Ltd., Tokyo, Japan) J-720 spectropolarimeter equipped with a temperature-controlled cell holder. Static measurements were recorded at 20 °C. Data from 3 scans were averaged using the software controlling the instrument. Secondary structure calculations were made using the Selcon software package (*21*).

Subunit Dissociation. Aliquots of eFSH and N[56]dg-eFSHα:eFSHβ were diluted to 10 μg/mL and incubated at 37 °C for 0, 1, 2, 4, 6, 16, 24, 48, and 72 h. After incubation, each sample was stored at 4 °C until all of the incubations were completed. The samples were then serially diluted with RLA buffer, and receptor-binding competition curves were determined in a rat testis FSH receptor assay, as described above. The relative potencies, a measure of subunit dissociation, were plotted against time and compared with previously reported data (*22*).

RESULTS

Oligosaccharide Characterization by MALDI−MS. Previous studies had suggested that the increase in the average αAsn[56] oligosaccharide mass in eFSHα and eCGα preparations over that of eLHα was due to the appearance of a second complex oligosaccharide branch in eFSHα and an extended form of this branch in eCGα (*11*). MS experiments were performed on Asn[56] oligosaccharide mixtures derived from eFSHα, eLHα, and eCGα, as well as partially fractionated eLHα Asn[56] oligosaccharides. Initially, MALDI mass spectra were obtained in the positive- and negative-ion modes for eFSHα, eLHα, and eCGα Asn[56] oligosaccharide mixtures (Figures 1−3). The resulting spectra were very complex, consisting of 34−78 ionic species representing at least 28−57 structures (Table 1 and Figure 4). Subsequently, MALDI−MS, MS/MS, and exoglycosidase digestions were employed to characterize 24 partially purified oligosaccharide fractions (Figure 5). Preparative high pH anion-exchange chromatography of 350 nmol of eLHα Asn[56] oligosaccharides produced essentially the same chromatogram as a 3 nmol sample fractionated on an analytical column (*10*). MALDI−MS indicated that only a few fractions, such as 2 and 6, were pure oligosaccharides. All other fractions were mixtures of 2−38 oligosaccharides. While this increased the number of oligosaccharide structures from at least 34 to 105, the Discussion in the present paper will be restricted to confirmation of the structures proposed on the basis of mass spectrometry of the oligosaccharide mixtures. The results confirmed previous oligosaccharide mapping experiments (*10*) that revealed a hormone-specific pattern of oligosaccharide heterogeneity associated with eLHα, eFSHα, and eCGα Asn[56] oligosaccharide populations (Figures 1−3). More detailed structural information was obtained regarding the oligosaccharides associated with each α subunit preparation (Table 1).

The oligosaccharide mixture isolated from eFSHα was the most heterogeneous. Its positive ion MALDI mass spectrum contained 74 ions ranging from *m*/*z* 771.3 to 2571.1. A total of 57 carbohydrate species were proposed on the basis of composition, consistent with the ion mass. Additional confirmatory data were obtained by MS/MS and exoglycosidase digestion. A total of 7 of these structures were detected in all 3 α subunit oligosaccharide preparations; 14 were present in both eLHα and eFSHα carbohydrate mixtures; and 7 were associated with both eFSHα and eCGα carbohydrate mixtures, while 29 were only found in eFSHα

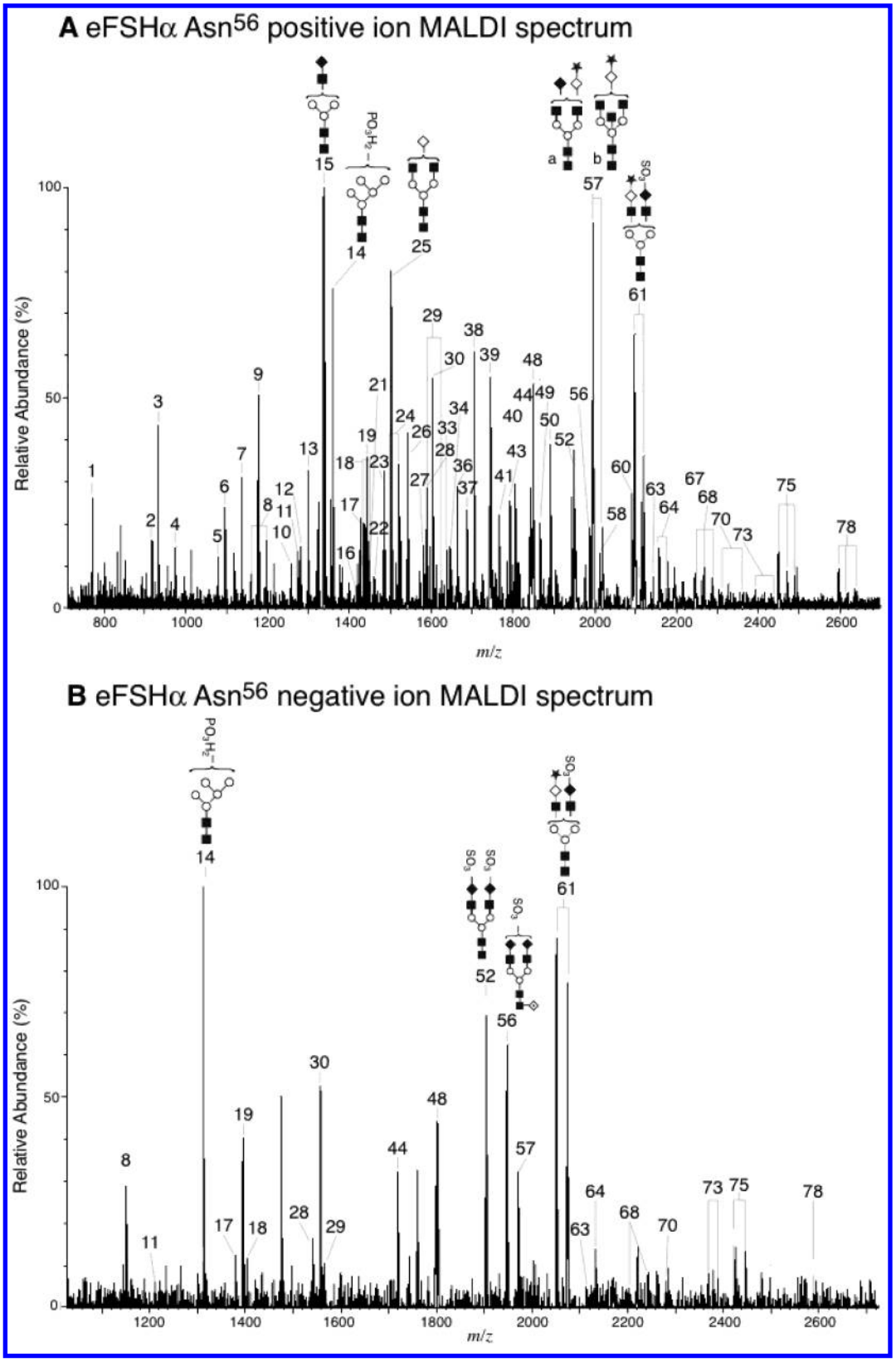

FIGURE 1: Analysis of eFSH αAsn[56] oligosaccharides by MALDI−MS. Samples of oligosaccharide released from α-subunit preparations by PNGase-F digestion were subjected to MS as described under the Materials and Methods. (A) eFSHα oligosaccharides, positive-ion mode. (B) Negative-ion mode. Symbols: ○ = mannose, ■ = *N*-acetylglucosamine, ◇ = galactose, ♦ = GalNAc, tilted ⊡ = fucose, ★ = *N*-acetylneuraminic acid, and ⊙ = an unknown substituent.

oligosaccharide mixtures. The most abundant oligosaccharides in the positive ion spectrometry for eFSHα were hybrid, high-mannose, and biantennary oligosaccharides, with some of the latter terminated with a single sialic acid residue (structures 14, 15, 25, 52, 56, 57, and 61 of Figure 1A). Two alternative structures were possible for oligosaccharide 15 (Figure 4) based on monosaccharide compositions that agreed with the *m*/*z* 1339.5 ion. However, only the preferred

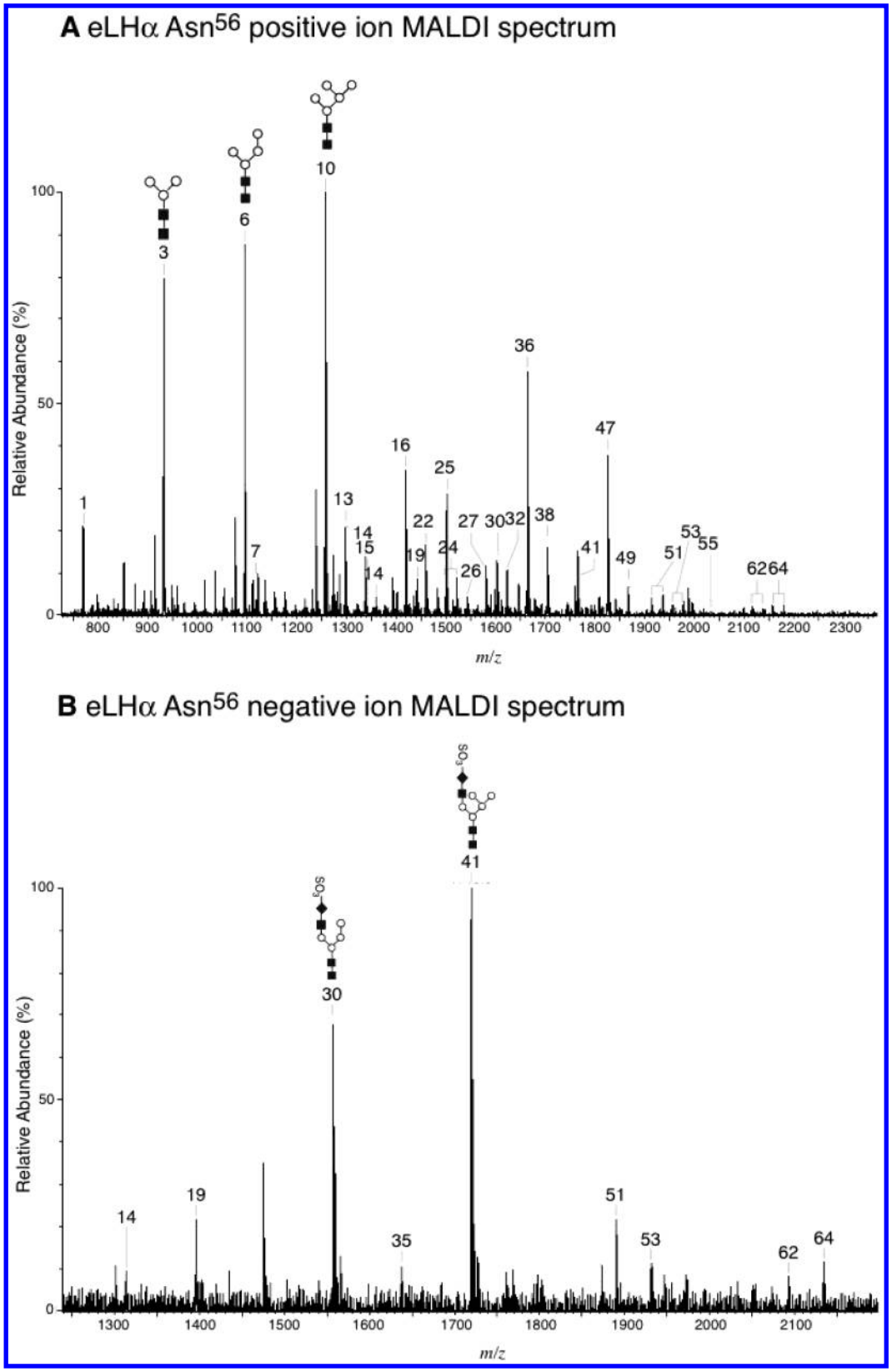

FIGURE 2: Analysis of eLH αAsn[56] oligosaccharides by MALDI−MS. Samples of oligosaccharide released from α-subunit preparations by PNGase-F digestion were subjected to MS as described under the Materials and Methods. (A) eLHα oligosaccharides, positive-ion mode. (B) Negative-ion mode. Symbols are the same as in the Figure 1 caption.

structure is shown in Figure 1A, because it also existed as a sulfated compound (*m*/*z* 1441.4, structure 19). The preferred alternative for structure 25 is shown because it also existed as its sialylated analogue (*m*/*z* 1792). In addition, the MS/MS spectrum did not contain an ion at *m*/*z* 429 $(HexNAc)_2$. Two alternatives labeled a and b are shown for structure 57, because no evidence supporting the existence of one over the other was obtained. Structure 57b was consistent with other abundant oligosaccharides in the mixture. Structure 61 was a biantennary oligosaccharide terminated with GalNAc-

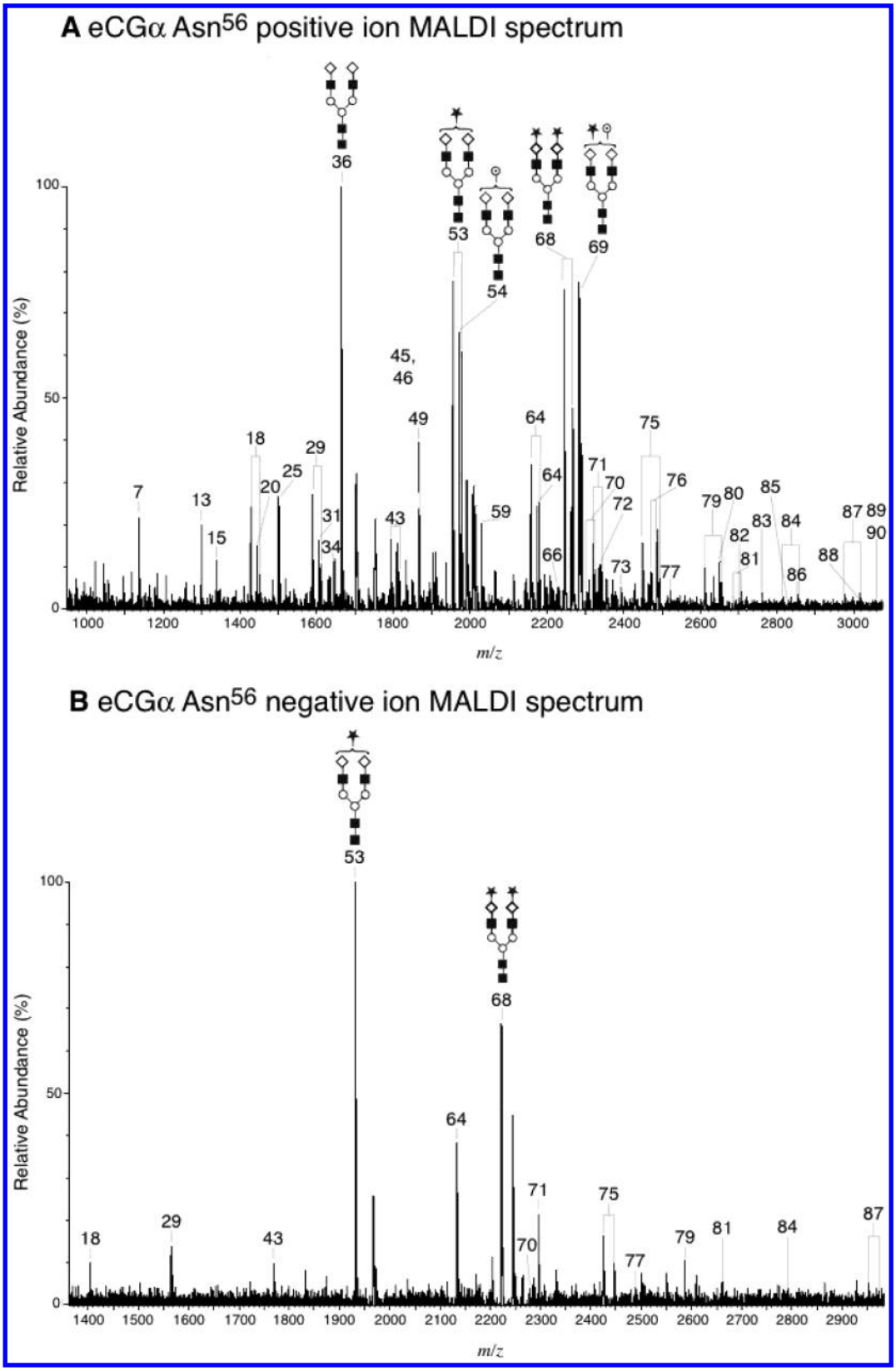

FIGURE 3: Analysis of eCG αAsn[56] oligosaccharides by MALDI−MS. Samples of oligosaccharide released from α-subunit preparations by PNGase-F digestion were subjected to MS as described under the Materials and Methods. (A) eCGα oligosaccharides, positive-ion mode. (B) Negative-ion mode. Symbols are the same as in the Figure 1 caption.

sulfate on one branch and sialic acid on the other and represented the oligosaccharide structure expected from the reported carbohydrate composition for eFSHα Asn[56] (*18*).

An unusual high-mannose oligosaccharide was among the more abundant eFSHα Asn[56] structures (structure 14). It appeared in both positive and negative ion MS experiments and was initially believed to represent a sulfated oligosaccharide but may well be phosphorylated, because this and related compounds appeared as both free acid as well as the sodium salt, while sulfated oligosaccharides appeared only

Table 1: Results from MALDI Analysis of ELHα, EFSHα, and ECGα Asn[56] Oligosaccharides

	mass				composition[f]							
	$[M + Na]^{+b}$		$[M - H]^{-d}$									
α subunit prep.[a]	found	calcd[c]	found	calcd[e]	Hex	HN	Fuc	Sial	X	SO_3	PO_3	footnotes[g]
1. F	771.3	771.3			2	2	0	0	0	0	0	*h*
L	771.4											
2. F	917.3	917.3			2	2	1	0	0	0	0	
3. F	933.2	933.3			3	2	0	0	0	0	0	*h*
L	933.2											
4. F	974.3	974.3			2	3	0	0	0	0	0	
5. F	1079.4	1079.4			3	2	1	0	0	0	0	
6. F	1095.4	1095.4			4	2	0	0	0	0	0	*i*
L	1095.3											
7. F	1136.3	1136.4			3	3	0	0	0	0	0	*j,k*
L	1136.4											
C	1136.3											
8. F	1175.3	1175.3	1151.3	1151.3	4	2	0	0	0	0	1	*l*
	1197.3	1197.3									1 (Na)	
9. F	1177.5	1177.4			2	4	0	0	0	0	0	
10. F	1257.4	1257.4			5	2	0	0	0	0	0	*i*
L	1257.3											
11. F	1279.4	1279.4	1233.4	1233.4	2	4	0	0	0	1 (Na)	0	
12. F	1282.5	1282.5			3	3	1	0	0	0	0	*m*
13. F	1298.6	1298.4			4	3	0	0	0	0	0	*k,n*
L	1298.4											
C	1298.4											
14. F	1337.5	1337.4	1313.4	1313.4	5	2	0	0	0	0	1	*o,p*
L	1337.5		1313.5									
F	1359.4	1359.4									1 (Na)	
L	1359.5											
15. F	1339.6	1339.5			3	4	0	0	0	0	0	*q,r,s*
L	1339.5											
C	1339.4											
16. F	1419.5	1419.5			6	2	0	0	0	0	0	*i*
L	1419.5											
17. F	1425.4	1425.4	1379.5	1379.5	2	4	1	0	0	1 (Na)	0	
18. F	1427.4	1427.5	1403.5	1403.5	3	3	0	1	0	0	0	
C	1427.3											
F	1449.5	1449.5						1 (Na)				
C	1449.4											
19. F	1441.5	1441.5	1395.2	1395.4	3	4	0	0	0	1 (Na)	0	*t,u*
L	1441.5		1395.4									
20. C	1443.4				3	3	0	0	1	0	0	*v*
21. F	1444.5	1444.5			4	3	1	0	0	0	0	
22. F	1460.5	1460.5			5	3	0	0	0	0	0	*w*
L	1460.5											
23. F	1485.6	1485.5			3	4	1	0	0	0	0	
24. F	1499.4	1499.5			6	2	0	0	0	0	1	*l,p*
L	1499.5											
F	1521.4	1521.4									1 (Na)	
L	1521.7											
25. F	1501.5	1501.5			4	4	0	0	0	0	0	*x,y,z*
L	1501.5											
C	1501.5											
26. F	1542.5	1542.6			3	5	0	0	0	0	0	*w,aa*
L	1542.6											
27. F	1581.5	1581.5			7	2	0	0	0	0	0	*i*
L	1581.5											
28. F	1587.5	1587.5	1541.5	1541.5	3	4	1	0	0	1 (Na)	0	
29. F	1589.5	1589.5	1565.6	1565.6	4	3	0	1	0	0	0	
C	1589.4		1565.5									
F	1611.6	1611.5						1 (Na)				
C	1611.5											
30. F	1603.5	1603.5	1557.6	1557.5	4	4	0	0	0	1 (Na)	0	*u,bb*
L	1603.5											
31. C	1605.4				4	3	0	0	1	0	0	*v*
32. L	1622.7	1622.6			6	3	0	0	0	0	0	*h*
33. F	1644.6	1644.6	1598.5	1598.5	3	5	0	0	0	1 (Na)	0	
34. F	1647.6	1647.6			4	4	1	0	0	0	0	
C	1647.6											
35. L	1661.6	1661.6	1637.5	1637.5	7	2	0	0	0	0	1	*p*
36. F	1663.6	1663.6			5	4	0	0	0	0	0	*cc,dd,ee*
L	1663.6											
C	1663.6											
37. F	1688.6	1688.6			3	5	1	0	0	0	0	*ff*
38. F	1704.6	1704.6			4	5	0	0	0	0	0	*gg,hh*
L	1704.7											
39. F	1745.6	1745.6			3	6	0	0	0	0	0	
40. F	1749.8	1749.6	1703.6	1703.5	4	4	1	0	0	1 (Na)	0	
41. F	1765.6	1765.5	1719.5	1719.5	5	4	0	0	0	1 (Na)	0	*w*
L	1765.6		1719.5									
42. F	1790.6	1790.6	1744.7	1744.6	3	5	1	0	0	1 (Na)	0	

Table 1: (Continued)

α subunit prep.[a]	mass [M + Na]$^{+b}$ found	mass [M + Na]$^{+b}$ calcd[c]	mass [M − H]$^{-d}$ found	mass [M − H]$^{-d}$ calcd[e]	composition[f] Hex	HN	Fuc	Sial	X	SO_3	PO_3	footnotes[g]
43. F	1796.2	1792.6	1768.6	1768.6	4	4	0	1	0	0	0	
C	1792.5		1768.7									
F	1814.7	1814.6						1 (Na)				
C	1814.6											
44. F	1806.6	1806.6	1760.6	1760.6	4	5	0	0	0	1 (Na)	0	*ii*
45. C	1808.6				4	4	0	0	1	0	0	*υ*
46. C	1809.6	1809.6			5	4	1	0	0	0	0	
47. L	1825.7	1825.6			6	4	0	0	0	0	0	*h*
48. F	1847.6	1847.6	1801.5	1801.6	3	6	0	0	0	1 (Na)	0	
49. F	1866.7	1866.7			5	5	0	0	0	0	0	*w,jj,kk,ll*
L	1866.8											
C	1866.7											
50. F	1891.7	1891.7			3	6	1	0	0	0	0	
51. L	1913.8	1913.7	1889.6	1889.7	6	3	0	1	0	0	0	*w*
	1935.8	1935.7						1 (Na)				
52. F	1949.5	1949.6	1903.6	1903.5	3	6	1	0	0	1 (Na)	0	
53. L	1954.8	1954.7	1930.7	1930.7	5	4	0	1	0	0	0	*w,mm*
C	1954.6		1930.6									*nn*
L	1976.7	1976.7						1 (Na)				
C	1976.6											
54. C	1970.6				5	4	0	0	1	0	0	*υ,oo*
55. L	1987.8	1987.7			7	4	0	0	0	0	0	*w*
56. F	1993.6	1993.6	1947.6	1947.7	3	6	1	0	0	1 (Na)	0	
57. F	1995.6	1995.7	1971.7	1971.7	4	5	0	1	0	0	0	
	2017.6	2017.7						1 (Na)				
58. F	2012.7	2012.7			5	5	1	0	0	0	0	
59. C		2028.7			6	5	0	0	0	0	0	*ll,pp,qq*
60. F	2095.5	2095.6	2151.6	2149.6	3	6	1	0	0	2 (Na)	0	
61. F	2097.6	2097.6	2051.6	2051.6	4	5	0	1	0	1 (Na)	0	
	2019.6	2019.6	2073.6	2073.6				1 (Na)				
62. L	2117.0	2116.7	2092.8	2092.7	6	4	0	1	0	0	0	*w*
	2138.9	2138.7						1 (Na)				
63. F	2141.7	2141.8	2117.6	2117.8	4	5	1	1	0	0	0	
64. F	2157.7	2157.7	2133.8	2133.7	5	5	0	1	0	0	0	*w,rr*
L	2157.9											
C	2157.7											
F	2179.7	2179.7						1 (Na)				*rr*
L	2179.9											
C	2179.7											
65. C	2173.7				5	5	0	0	1	0	0	*ll,rr*
66. C	2231.8	2231.8			6	6	0	0	0	0	0	*qq,rr*
67. F	2243.6	2243.7			4	5	1	1	0	1 (Na)	0	
68. F	2245.6	2245.8	2221.6	2221.8	5	4	0	2	0	0	0	
C	2245.8		2221.7									
F	2267.7	2267.8	2243.5	2243.8				2 (Na)				
C	2267.8		2243.7									
F	2289.5	2289.8						2 $(Na)_2$				
C	2289.8											
69. C	2261.7	2261.7			5	4	0	1	0	0	0	
	2283.7	2283.7										
70. F	2303.8	2303.8	2279.7	2279.8	5	5	1	1	0	0	0	*qq*
C	2303.7		2279.7									
F	2325.7	2325.8						1 (Na)				
C	2325.8											
71. C	2319.8	2319.8	2295.7	2295.8	6	5	0	1	0	0	0	*qq,rr*
	2341.8	2341.8						1 (Na)				
72. C	2335.8				6	5	0	0	1	0	0	*qq,rr*
73. F	2391.6	2391.8	2367.7	2367.8	5	4	1	2	0	0	0	
	2435.7	2435.8	2389.1	2389.8				2 $(Na)_2$				
74. C	2393.9	2393.8			7	6	0	0	0	0	0	*ss*
75. F	2448.7	2448.8	2424.8	2424.8	5	5	0	2	0	0	0	*qq*
C	2448.9		2424.6									
F	2470.8	2470.8	2446.9	2446.8				2 (Na)				
C	2470.9		2446.6									
F	2492.7	2492.8						2 $(Na)_2$				
C	2492.9											
76. C	2465.0				5	5	0	1	1	0	0	*qq*
	2486.7							1 (Na)				*qq*
77. C	2522.8	2522.9	2489.8	2489.9	6	6	0	1	0	0	0	
78. F	2594.8	2594.9	2571.1	2570.9	5	5	1	2	0	0	0	
	2616.6	2616.9	2592.7	2592.7				2 (Na)				
	2638.6	2638.9						2 $(Na)_2$				
79. C	2611.0	2610.9	2586.9	2586.9	6	5	0	2	0	0	0	*qq*
	2632.9	2632.9						2 (Na)				*qq*
	2655.0	2654.9						2 $(Na)_2$				*qq*
80. C	2626.7				6	5	0	1	1	0	0	*qq*
	2648.8							1 (Na)				*qq*

Table 1: (Continued)

α subunit prep.[a]	mass [M + Na]+[b] found	mass [M + Na]+[b] calcd[c]	mass [M − H]−[d] found	mass [M − H]−[d] calcd[e]	composition[f] Hex	HN	Fuc	Sial	X	SO_3	PO_3	footnotes[g]
81. C	2684.7	2684.9	2660.8	2660.9	7	6	0	1	0	0	0	*ss*
	2706.7	2706.9						1 (Na)				*ss*
82. C	2701.3				7	6	0	0	1	0	0	*ss*
83. C	2759.0	2759.0			8	7	0	0	0	0	0	*tt*
84. C	2814.1	2814.0	2789.6	2790.0	6	6	0	2	0	0	0	
	2836.7	2836.0						2 (Na)				
	2857.9	2857.9						2 $(Na)_2$				
85. C	2830.6	2831.0			7	6	1	1	0	0	0	*ss*
86. C	2851.8				6	6	0	1 (Na)	0	0	0	
87. C	2976.6	2976.0	2952.0	2952.0	7	6	0	2	0	0	0	*ss*
	2998.2	2998.0	2974.4	2974.0				2 (Na)				
	3019.8	3020.0						2 $(Na)_2$				
88. C	3014.9				7	6	0	1 (Na)	1	0	0	*tt*
89. C	3050.9	3050.1			8	7	0	1	0	0	0	*tt*
	3072.8	3072.1						1 (Na)				
90. C	3066.5				8	7	0	0	1	0	0	*tt*

[a] The numeral indicates the structure shown in Figure 4. The letter indicates the subunit oligosaccharide mass spectrum in which the ion was detected: F = eFSHα (Figure 1), L = eLHα (Figure 2), and C = eCGα (Figure 3). [b] Mass of $[M + Na]^+$ ion. [c] Calculated mass of $[M + Na]^+$ ion. Actual mass did not differ by >0.2 mass units. [d] Mass of $[M - H]^-$ or $[M - Na]^-$ ion. [e] Calculated mass of $[M - H]^-$ or $[M - Na]^-$ ion. All experimental results were within 0.2 mass units of the calculated values. [f] Hex = hexose (mannose and galactose), HN = *N*-acetylhexosamine (GlcNAc and GalNAc), Fuc = deoxyhexose (assumed to be fucose), Sial = sialic acid, X = unknown substituent (This substituent appeared at 16 mass units above that of each glycan containing Neu5Ac substituents. It was first assumed to be the corresponding *N*-glycolyl-sialic acid because that has been reported as a component of eCG*β* Asn[13] oligosaccharides (Damm, 1990, 438). However, this substituent was not acidic because it did not give a negative ion spectrum or form a sodium salt as expected. It did not appear to be a potassium adduct/salt, which would also increase the mass by 16. A recent MALDI−MS/MS spectrum on three of these compounds showed losses of 291 mass units corresponding to sialic acid. However, many other ions in the spectra were not the normal glycan ions, suggesting that these compounds may be artifacts. Nevertheless, we have listed them in the table because they appear to accompany the normal sialic acids.), SO_3 = sulfate, and PO_3 = phosphate. [g] No reasonable compositions were found for ions not listed. [h] MS/MS spectrum consistent with the structure during analysis of eFSHα oligosaccharides. [i] MS/MS spectrum consistent with the structure during analysis of eLHα oligosaccharides. The compound was not sensitive to galactosidase, fucosidase, or *Streptococcus pneumoniae β-N*-acetylhexosaminidase but was digested by Jack bean α-mannosidase. [j] For eFSHα and eCGα oligosaccharides, the lower structure (structure 7 of Figure 4) was preferred. A compound having a composition corresponding to the sialylated analogue of this glycan was also found, suggesting the occurrence of the lower structure in Figure 4. A metastable ion at *m*/*z* 1176 (calcd 1176.6) representing the loss of sialic acid indicated that this compound had the same core structure as *m*/*z* 1427.3, and therefore, the lower structure was present (*41*). There was no evidence for the presence of the other structure. [k] No MS/MS data for eLHα oligosaccharides. The compound was sensitive to *S. pneumoniae β-N*-acetylhexosaminidase confirming nonreducing terminal GlcNAc and suggesting that the upper structure was present on this hormone. [l] Comments largely derived from analysis of fraction 14 of Figure 5A. The mass of this glycan is 80 above that of *m*/*z* 1095, and like other glycans in this fraction, it forms a sodium salt (*m*/*z* 1197.4). Compounds showing the same behavior in the eFSHα oligosaccharide sample gave negative ions confirming the presence of an anionic group (a negative ion spectrum has not yet been run on fraction 14). This mass shift suggested the presence of sulfate or phosphate (both add the same nominal mass). All of the glycans in this fraction behaved similarly with respect to sodium salt formation, suggesting that they were all substituted with the same acidic group. They were also present in later fractions (e.g., fractions 15 and 16) as mixtures of free acid and sodium salt, along with other compounds that formed only sodium salts. These latter compounds were clearly sulfates by comparison with similar compounds seen in other samples, and we have only seen sulfates as their sodium salts in MALDI spectra. This observation suggested that the compounds present in this fraction were not sulfates but phosphates. Support for this conclusion was provided by peaks from the more abundant compounds that appear to be disodium salts (e.g., *m*/*z* 1543.2 from the free glycan at *m*/*z* 1499.5). Sulfates would not show this behavior. Also, phosphated high mannose glycans have been reported before. This conclusion was checked by testing the susceptibility of the glycans in fraction 15 of Figure 5A toward phosphatase. Two peaks, *m*/*z* 1441.4 and *m*/*z* 1587.5, disappeared after digestion for 7 h with alkaline phosphatase, while two minor peaks (*m*/*z* 1257.4 and *m*/*z* 1419.5) increased in abundance, indicating the loss of one phosphate. The MS/MS spectrum of the free acid (*m*/*z* 1175) showed peaks for Man + 80 and $(Man)_2$ + 80, indicating that the phosphate was located on mannose. A peak at *m*/*z* 609.4 $[(Man)_1(GlcNAc)_2]$ had a peak 80 mass units above, suggesting substitution on the core mannose. However, this latter peak was very weak in the spectra of the other compounds. [m] The lower structure was preferred because the compound also exists as its sialylated analogue (*m*/*z* 1589) as explained in footnote *j*. It is possibly a mixture of both structures. [n] For eCGα oligosaccharides, a metastable ion at *m*/*z* 1337 (calcd 1337.8) representing the loss of sialic acid indicated that this compound had the same core structure as *m*/*z* 1589.4 (structure 29 of Figure 4). [o] The structure was consistent with eFSHα oligosaccharide MS/MS data, digests with mannosidase. [p] Weak ion is in positive mode, and stronger ion is in negative mode. It forms a free acid and sodium salt and is probably a phosphate (see footnote *l*). [q] The upper structure was preferred for eFSHα oligosaccharides because the compound also exists as its sulfated analogue (*m*/*z* 1441.4). [r] MS/MS spectrum ambiguous for eLHα oligosaccharides, probably a mixture of isomers. [s] The presence of complex structures in the eCGα oligosaccharide sample and the sensitivity of the compound to *S. pneumoniae N*-acetylhexosaminidase in this fraction suggests that this compound has the top structure. [t] Structure consistent with eFSHα oligosaccharide MS/MS data. [u] No eLHα oligosaccharide MS/MS data. The structure is based on the formation of sulfate. [v] The eCGα compound digests with sialidase, suggesting that ⊙ is some kind of sialic acid, although it does not show acidic properties (see footnote *f* above). [w] No MS/MS data (for eLHα oligosaccharide sample). [x] For eFSHα, the lower structure is preferred because the compound also exists as its sialylated analogue (*m*/*z* 1792). Also, MS/MS spectrum does not contain an ion at *m*/*z* 429 $(HexNAc)_2$. [y] For eLHα, MS/MS data and exoglycosidase sequencing (partial sensitivity to bovine testis *β*-galactosidase and partial insensitivity to *β*-galactosidase and *S. pneumoniae β-N*-acetylhexosaminidase) suggest that this compound has mainly the top structure (structure 25 of Figure 4). [z] For eCGα oligosaccharides, a metastable ion at *m*/*z* 1540 (calcd 1539.7) representing the loss of sialic acid indicates that this compound has the same core structure as *m*/*z* 1792.5. [aa] The compound forms a sulfated analogue (*m*/*z* 1644), in eFSHα oligosaccharides; therefore, the upper structure (structure 26 of Figure 4) is present. It is also consistent with MS/MS data. [bb] The structure is consistent with eFSHα oligosaccharide MS/MS data (ions at *m*/*z* 531 $[(HexNAc)_2-SO_3Na]$ and 671 $[(Man)_4]$. [cc] In eFSHα oligosaccharide mixture, both the top and bottom structures are probably present because both sulfated and sialylated analogues are present in the sample. [dd] MS/MS data and results from exoglycosidase sequencing eLHα oligosaccharides indicate that this compound has mainly the top structure with a little of the middle one (structure 36 of Figure 4). [ee] For eCGα oligosaccharides, the middle structure is preferred. Metastable ions at *m*/*z* 1701.5 and 1752.3 (calcd 1700.9 and 1751.4, respectively) representing the loss of one and two sialic acids, respectively, indicates that this compound has the

Table 1: (Continued)

same core structure as *m*/*z* 1954.6 and 2245.8. [ff] The sulfated analogue is present at *m*/*z* 1790 providing evidence for the upper structure (structure 37 of Figure 4). [gg] Both sulfated and sialylated analogues are present, providing evidence for both structures in the eFSHα oligosaccharide mixture. [hh] The compound in eLHα oligosaccharide mixture is sensitive to bovine testis β-galactosidase showing the presence of nonreducing terminal galactose. MS/MS spectrum is consistent with the lower structure (structure 38 of Figure 4). There is no ion at *m*/*z* 429 (therefore, no structure with the GalNAc-GlcNAc chain). [ii] The structure is consistent with MS/MS data. [jj] There are no MS/MS data for the eLHα oligosaccharide mixture. The upper structure (structure 49 of Figure 4) is consistent with MS/MS data for eFSHα oligosaccharides. An ion at *m*/*z* 694 suggests the presence of a bisecting GlcNAc. [kk] For eCGα oligosaccharides, a metastable ion at *m*/*z* 1903 (calcd 1903.3) representing the loss of sialic acid indicates that the compound has the same core structure as *m*/*z* 2157.7 (structure 64 of Figure 4). [ll] Only one of two possible isomers for the triantennary glycan is shown (determination as to which isomer is present can be made by exoglycosidase digestion). The observation that a potential triantennary compound in fraction 11 (Figure 5) may have a branched 6 antenna may be relevant. However, both structures may exist. [mm] A metastable ion at *m*/*z* 1990 (calcd 1990.9) representing the loss of sialic acid indicates that this compound has the same core structure as *m*/*z* 2245.8. [nn] A metastable ion at *m*/*z* 2012.4 (calcd 2012.5) representing the loss of sialic acid indicates that this compound has the same core structure as *m*/*z* 2267.8. [oo] A metastable ion at *m*/*z* 2006 (calcd 2006.8) representing the loss of sialic acid indicates that this compound has the same core structure as *m*/*z* 2261.7. The ⊙ group is stable, reflecting its nonacidic nature. [pp] A metastable ion at *m*/*z* 2064 (calcd 2064.7) representing the loss of sialic acid indicates that this compound has the same core structure as *m*/*z* 2319.8. [qq] Digestion with bovine testis β-galactosidase gives both $(Hex)_3(HexNAc)_5$ and $(Hex)_4(HexNAc)_5$, indicating that this compound is a mixture of a triantennary glycan and a biantennary glycan with a *N*-acetyllactosamine extension. Ion series *m*/*z* 2448.7, 2470.8, 2492.6 were present in the eLH mass spectrum but not in the eCG mass spectrum. However, because these are disialylated compounds, their absence from the negative ion spectrum of eCG spectrum is probably due to fragmentation and is not structurally significant. [rr] A metastable ion links this compound to its sialylated analogue. [ss] Digestion with bovine testis β-galactosidase gives both $(Hex)_4(HexNAc)_6$ and $(Hex)_5(HexNAc)_6$, indicating that this compound is a mixture of a triantennary glycan and a biantennary glycan with a *N*-acetyllactosamine extension. [tt] Digestion with bovine testis β-galactosidase gives both $(Hex)_5(HexNAc)_7$ and $(Hex)_6(HexNAc)_7$, indicating that this compound is a mixture of a triantennary glycan with two *N*-acetyllactosamine extensions and a biantennary glycan with three extensions.

as sodium salts. Digestion with alkaline phosphatase confirmed the presence of phosphate (data not shown). The compound was digested with mannosidase, indicating high-mannose structure, and structure 14 was consistent with MS/MS data. A similar, although less abundant, compound was noted in the eLHα Asn^{56} oligosaccharides, and analysis of partially purified oligosaccharide fractions 14−16 (Figure 5A) revealed several polyphosphorylated high-mannose oligosaccharides among the more abundant species. The MS/MS spectrum of the free acid (*m*/*z* 1337.5) showed the absence of the phosphate on the reducing-terminal GlcNAc and its presence on one of the mannose residues. The MS/MS spectrum of the sodium salt was not only complicated (nearly 100 peaks) but also indicated that the location of the phosphate was on a mannose residue near the core of the glycan (several sites may, of course, be occupied). The similarity between the lower mass range of this spectrum and those of the other sodium salts supported this deduction and indicated that all of these glycans were substituted at common positions. The potentially phosphorylated oligosaccharide (structure 14) provided the most abundant ion in the negative ion spectrum (Figure 1B). Three other abundant ions indicated the presence of two other biantennary, sulfated oligosaccharides (structures 52 and 56, as well as structure 61).

The oligosaccharide mixture isolated from eLHα initially appeared the least heterogeneous, consisting of 34 ions, representing 28 oligosaccharide species ranging from *m*/*z* 771.3 to 2157.7. Of these, 6 were unique to eLHα. Additional confirmatory data were obtained by MS/MS and exoglycosidase digestion applied to the oligosaccharide mixture as well as the 24 partially fractionated samples. For eLHα, the most abundant positive ions were small high-mannose structures. In most cases, these consisted of the pentasaccharide core alone (structure 3) or with an additional one or two mannose residues (structures 6 and 10 of Figure 2A). This result was consistent with chromatographic data (Figure 5B), because the bulk of the carbohydrate was recovered from fractions 4−8, which were composed of these high-mannose oligosaccharides. In the negative ion MALDI spectrum, hybrid complex/sulfated, high-mannose oligosaccharides (structures 30 and 41) that differed in the number of mannose residues on the α1−6 branch were the most abundant compounds. While hybrid oligosaccharides were the most abundant type associated with this glycosylation site in oLHα and hCGα (*23*, *24*), in eLHα, they were less abundant than the high-mannose type (Figure 5B).

The oligosaccharide mixture isolated from eCGα consisted of 63 ions, representing 41 oligosaccharide species ranging from *m*/*z* 1136.4 to 3066.5. Of these, 26 were unique to eCGα. The chief difference between pituitary gonadotropin and placental eCG glycosylation was the absence of high-mannose or hybrid structures in the latter as indicated by exoglycosidase digestion. All compounds derived from eCG digested to $(GlcNAc)_2(Man)_2$ or $(GlcNAc)_2(Man)_3$ with a mixture of sialidase, β-galactosidase, and *S. pneumoniae* *N*-acetylhexosaminidase. They were insensitive to mannosidase, indicating that they all had complex rather than hybrid or high-mannose structures. Two of the most abundant ions in the positive and negative ion spectra for eCGα oligosaccharides (structures 53 and 68 of Figure 3) represented the same biantennary oligosaccharide core that was terminated with one or two sialic acid residues, with one sialic acid or one possible derivative of sialic acid, although negative ion data for the latter were lacking (footnote *d* of Table 1) or one of each. The most abundant ion (*m*/*z* 1663.6, structure 36) was present in eLHα and eFSHα oligosaccharide mixtures but represented hybrid oligosaccharide structures in those hormones (Figure 4). The structure shown for eCGα was biantennary and related to the other major oligosaccharides associated with this site, although lacking both sialic acid residues. Larger ions representing triantennary oligosaccharides or oligosaccharides extended with lactosamine repeats were present in lower abundance.

Receptor-Binding Activities of eLH and eFSH Hybrid Hormone Preparations. All subunit combinations produced functional heterodimer preparations that were active in LH and/or FSH receptor-binding assays (Figure 6). Elimination of αAsn^{56} carbohydrate produced a 39−75% increase in apparent LH receptor-binding activity for the eLHβ hybrid derivatives and a larger, 2−5-fold increase in FSH receptor-binding activity (Tables 2 and 3). Either no change or a 23−

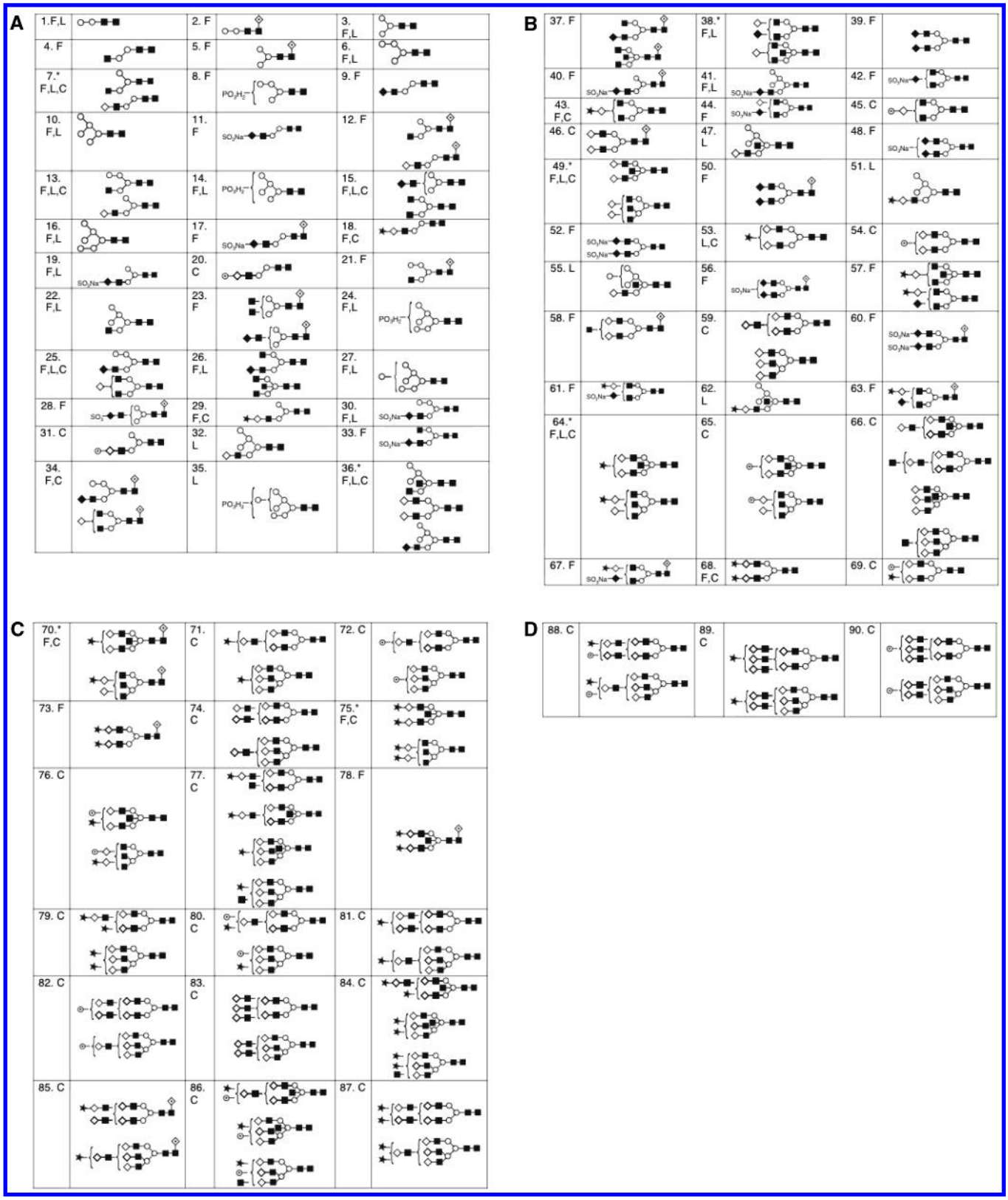

FIGURE 4: Oligosaccharide structures based on MS data shown in Figures 1−3 and documented in Table 1. The numbers associated with each structure correspond to column 1 of Table 1. Structures for eFSH, eLH, and eCG oligosaccharides (F, L, and C, respectively) were based on mass, MS/MS, and exoglycosidase data. For eCG oligosaccharides, all compounds were digested to $(GlcNAc)_2(Man)_2$ or $(GlcNAc)_2$-$(Man)_3$ with a mixture of sialidase, β-galactosidase, and *S. pneumoniae N*-acetylhexosaminidase. They were insensitive to mannosidase, indicating that they all had complex rather than hybrid or high-mannose structures. Symbols: ○ = mannose, ■ = *N*-acetylglucosamine, ◇ = galactose, ♦ = GalNAc, tilted ⊡ = fucose, ★ = *N*-acetylneuraminic acid, and ⊙ = an unknown substituent.

26% reduction in FSH receptor-binding activity accompanied αAsn[56] deglycosylation of eFSHβ hybrid preparations.

To determine if a carbohydrate inhibited receptor binding by directly interfering with hormone-receptor interaction or

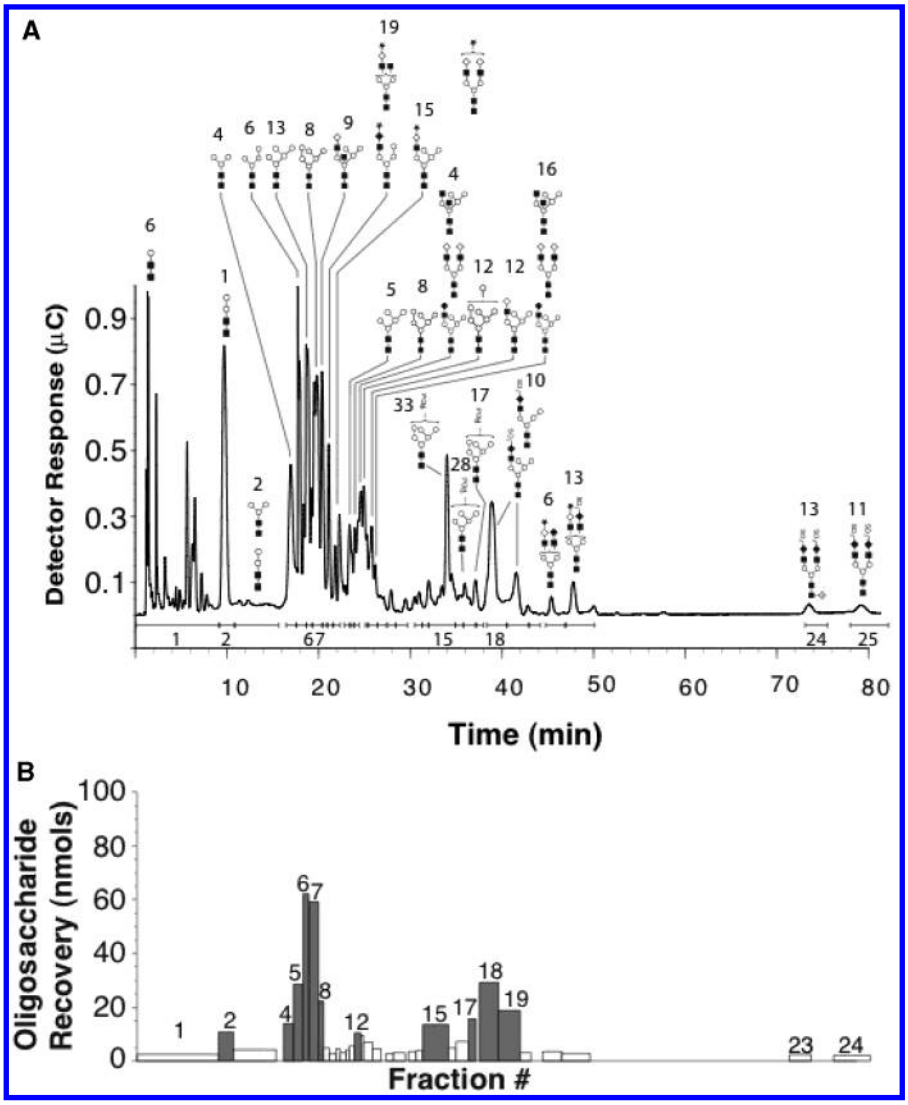

FIGURE 5: Preparative fractionation of 350 nmol of eLHα Asn^{56} oligosaccharides. (A) High pH anion-exchange chromatography using a Dionex carbohydrate analyzer. The 1−3 most abundant oligosaccharide structure(s) are shown for each fraction. Symbols: ○ = mannose, ■ = *N*-acetylglucosamine, ◇ = galactose, ♦ = GalNAc, tilted ⊡ = fucose, ★ = *N*-acetylneuraminic acid, and ⊙ = an unknown substituent. (B) Oligosaccharide yield. Bar width shows portion of the chromatogram pooled to obtain the fraction. Bar height indicates the amount of oligosaccharide estimated by carbohydrate analysis of 4 N TFA hydrolysates.

indirectly by charge repulsion between the negatively charged terminal sulfate or sialic acid moieties and the negatively charged membrane surface, we performed an LH receptor-binding assay using a detergent-solubilized membrane preparation. Competition of eLHβ hybrids for ^{125}I-hCG binding to solubilized rat testis LH receptors showed the same pattern of reduced LH receptor binding with increased αAsn^{56} oligosaccharide size as was observed with crude membrane preparations (Figure 7). Thus, the reduction in receptor-binding activity represented oligosaccharide inhibiting hormone-receptor interaction and not nonspecific repulsion of negatively charged oligosaccharide termini and negatively charged membrane components.

CD. The influence of altered oligosaccharide structure on gonadotropin conformation was assessed by using CD to measure secondary structure in intact and Asn^{56}-deglycosylated eLH and eFSH hybrid preparations. CD measurements for six eLH hybrids were compared with that of eLH (Figure 8). Two intact α-subunit hybrid preparations, eFSHα:eLHβ and eCGα:eLHβ, exhibited very similar CD spectra to each other and that of intact eLH, while that of eLHα:eLHβ differed. The latter exhibited increased α-helical content and decreased β-sheet content as compared with native eLH (Table 2). Elimination of αAsn^{56} oligosaccharide produced hybrids that exhibited more variable CD spectra. That is, all three partially deglycosylated eLH hybrid derivative spectra differed from each other rather than exhibiting a single intact α hybrid spectrum as expected. Changes in secondary structure varied for each pair of intact- and N^{56}dg-α hybrid preparation. Thus, for eLHα:eLHβ, the increased α-helix and reduced β-strand contents were reduced and increased, respectively, following Asn^{56} deglycosylation, so that they were now similar to intact eLH. For eFSHα hybrids, there was little change in α-helical or β-strand contents following Asn^{56} deglycosylation, instead the β-turn content and random secondary structure increased. The former suggested an altered conformation in loops L1 and L3. For the eCGα hybrids, Asn^{56} deglycosylation was associated with increased helical and decreased β-strand content, similar to what was associated with eLHα:eLHβ; however, the increased LH

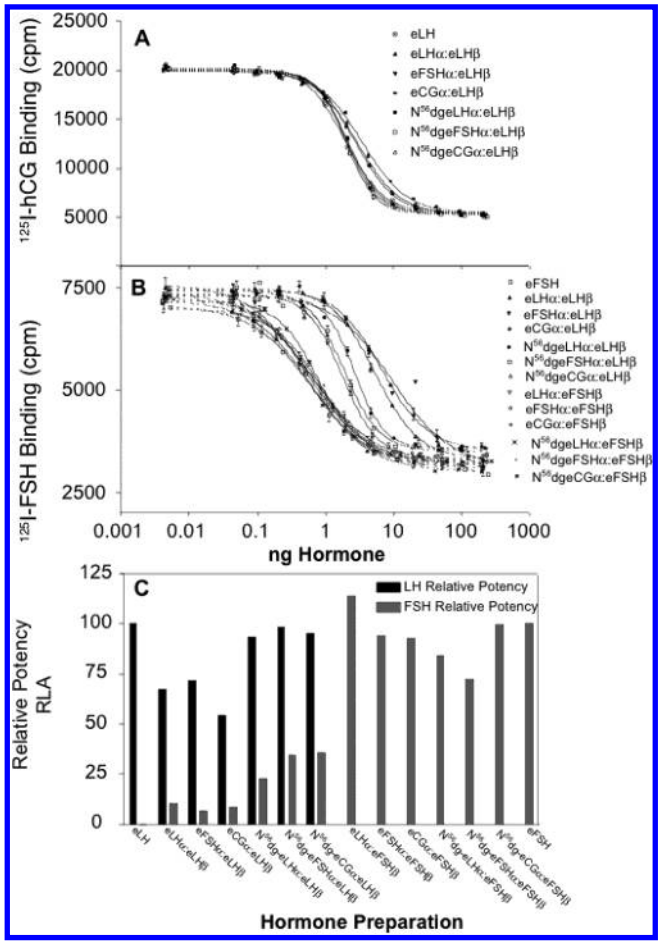

FIGURE 6: Radioligand receptor assays of hybrid hormone preparations employed in this study. (A) LH radioligand assay using rat testis homogenate and LH receptor-specific ^{125}I-hCG tracer. Because only LH preparations bind LH receptors, FSH hybrids were not included. (B) FSH radioligand assay using rat testis homogenate and ^{125}I-eFSH tracer. (C) Relative potencies derived from the competition curves in A and B.

receptor-binding activity resulting from removing this oligosaccharide was unaffected and was identical to those of N[56]dg-eLHα:eLHβ and N[56]dg-eFSHα:eLHβ.

For eFSHβ hybrids, the intact hybrid hormone preparations exhibited nearly identical CD spectra, as expected. The secondary structure estimates were similar to those for eFSH, except for a reduced β-sheet content. The αAsn[56]-deglycosylated FSH hybrid CD spectra, however, differed from each other (Figure 9). Changes in secondary structure associated with removal of a carbohydrate varied from preparation to preparation (Table 3). Thus, increased α-helix and reduced β-sheet contents were associated with N[56]dg-eLHα:eFSHβ. Only increased α-helical content was noted for N[56]dg-eFSHα:eFSHβ, while the N[56]dg-eCGα:eFSHβ secondary structure was relatively unchanged. In the case of the latter hybrid, receptor-binding activity was not reduced by the absence of αAsn[56] carbohydrate, consistent with a secondary structure very similar to that of eFSH. The other two hybrids, N[56]dg-eLHα:eFSHβ and N[56]dg-eFSHα:eFSHβ, exhibited a reduction in FSH receptor-binding activity despite the elimination of this oligosaccharide, possibly as a result of subunit dissociation.

Because the CD spectral changes accompanied by reduced FSH receptor-binding activity suggested subunit dissociation, we repeated an earlier experiment, using the loss of FSH receptor-binding activity as a dissociation indicator (*22*). Incubation of intact eFSH and N[56]dg-eLHα:eFSHβ (the preparation showing the largest change in CD spectrum) at 37 °C for up to 144 h, revealed a progressive, 50% loss of FSH receptor-binding activity for intact eFSH after 72 h, similar to previous results (Figure 10). A more rapid loss of activity was associated with N[56]dg-eLHα:eFSHβ over the first 6 h, followed by a progressive recovery of binding activity during subsequent incubation intervals. After 2 h, a 35% loss of binding activity was noted, somewhat greater than the 23−26% reduction in the activities of the Asn[56]-deglycosylated derivatives of eFSHα:eFSHβ and eLHα:eFSHβ, respectively. However, the stability study actually involved a longer incubation time when the preincubation for 2 h and assay incubation for 2 h are both taken into account.

DISCUSSION

The common α subunit has generally been considered interchangeable between glycoprotein hormone preparations. However, hormone-specific glycosylation produces unique α subunits. Because these subunit preparations are readily isolated from heterodimer preparations and reassociated with β-subunit preparations, these α-subunit glycoforms are valuable tools for studying the mechanisms by which carbohydrate alters hormonal activity, provided the oligosaccharide structures can be characterized. Reduced LH receptor binding as the αAsn[56] oligosaccharide size increased was observed when potential cell membrane effects were eliminated by using solublized LH receptor preparations. Although this demonstrated that oligosaccharide specifically inhibited LH−receptor interactions, both steric hindrance and conformational change remained potential mechanisms to explain the reduction in receptor-binding affinity. CD studies revealed that conformational changes occurred whenever αAsn[56] oligosaccharide was removed. For intact eFSH

Table 2: Selcon Analysis of ELH Hybrid CD Spectra and Results of LH and FSH Receptor-Binding Assays

	secondary structure estimates from CD				FSH RLA		LH RLA	
hormone preparation	α helix	β sheet	β turn	other	relative potency	95% CL	relative potency	95% CL
eLH	12.2	41.0	26.2	20.9	ND[a]		100	82.0−122.0
eLHα:eLHβ	16.8	34.1	27.3	22.1	10.6	8.4−13.3	67.3	57.0−79.4
eFSHα:eLHβ	13.4	40.3	27.7	21.6	6.5	4.8−8.9	71.6	59.8−85.8
eCGα:eLHβ	13.5	37.8	29.1	18.1	8.5	6.9−10.4	54.7	47.2−63.5
N[56]dg-eLHα:eLHβ	11.3	39.4	26.7	24.1	23.0	16.7−31.9	93.8	73.6−119.7
N[56]dge-FSHα:eLHβ	11.4	40.6	24.7	24.1	34.6	26.1−45.8	98.5	73.0−133.0
N[56]dg-eCGα:eLHβ	17.2	33.3	27.2	20.4	35.6	27.2−46.7	95.2	71.3−127.3

[a] ND = not determined.

Table 3: Selcon Analysis of EFSH Hybrid CD Spectra and Results of FSH Receptor-Binding Assays

	secondary structure estimates from CD				FSH RLA		LH RLA	
hormone preparation	α helix	β sheet	β turn	other	relative potency	95% CL	relative potency	95% CL
eFSH	17.4	29.1	25.7	27.1	100	84.5−118.4	ND[a]	ND
eLHα:eFSHβ	18.8	23.9	27.3	28.9	114.1	103.8−125.4	ND	ND
eFSHα:eFSHβ	18.5	24.0	27.1	29.0	94.1	81.9−108.2	ND	ND
eCGα:eFSHβ	18.6	23.5	26.8	28.5	92.6	80.0−107.1	ND	ND
N^{56}dg-eLHα:eFSHβ	30.9	20.3	27.1	25.5	84.5	69.2−103.2	ND	ND
N^{56}dg-eFSHα:eFSHβ	21.1	25.4	28.4	28.9	72.7	62.7−84.4	ND	ND
N^{56}dg-eCGα:eFSHβ	17.3	24.1	26.8	28.9	99.5	88.3−112.2	ND	ND

[a] ND = not determined.

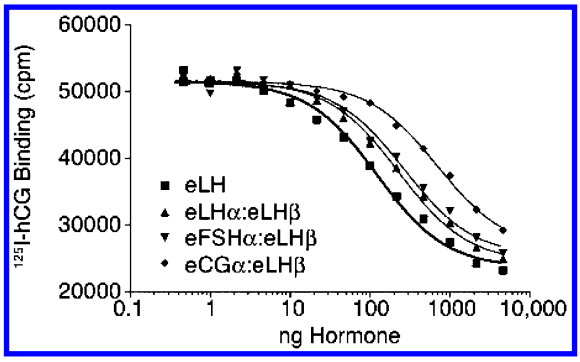

FIGURE 7: Radioligand receptor assay using solubilized rat testis LH receptors and ^{125}I-hCG tracer.

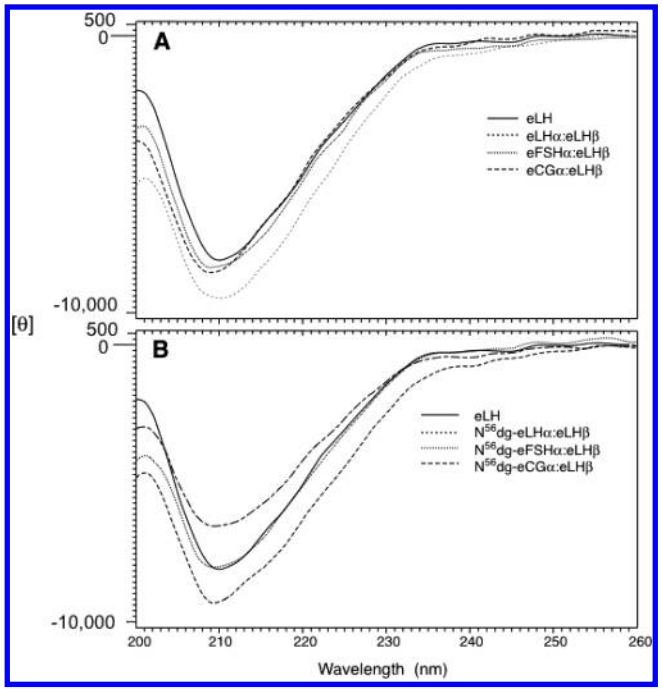

FIGURE 8: CD of eLHβ hybrids. (A) Intact hybrids, as indicated. (B) αAsn^{56}-deglycosylated hybrids.

hybrids, the conformation remained essentially the same, while in the case of the eLH hybrids, the conformation of eLHα:eLHβ differed from those of eFSHα:eLHβ and eCGα:eLHβ. Increased α-helix and reduced β-strand contents estimated from CD spectra, suggested conformational changes may have been restricted to α-subunit long loop L2 because the only consensus helical region in hCG and hFSH was located in αL2 (*25*−*27*). However, this will have to be examined further using methods that can define conformation in specific regions of the hormone. Because carbohydrate

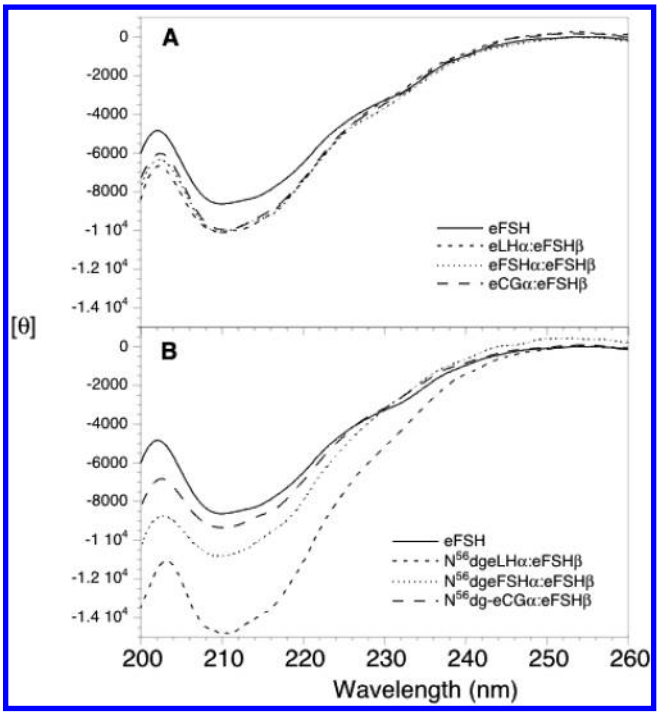

FIGURE 9: CD of eFSHβ hybrids. (A) Intact hybrids. (B) αAsn^{56}-deglycosylated hybrids.

also inhibited receptor binding by steric hindrance, it was essential to better characterize the oligosaccharide structures present at αAsn^{56}.

The present study employed MALDI−MS to provide greater structural detail for the oligosaccharide populations associated with equine gonadotropin α-subunit preparations. Our earlier oligosaccharide mapping studies had suggested considerable structural heterogeneity in equine gonadotropin αAsn^{56} oligosaccharide populations (*10*). On the basis of retention times, monosaccharide composition, and an average mass of 1482 inferred from comparisons of the masses of intact and Asn^{56}-deglycosylated α-subunit preparations, we suggested that hybrid-sulfated oligosaccharides, varying in the number of mannose residues, were the most abundant structures in eLHα (*11*), similar to those attached to oLHα and hCGα at the equivalent position (*23*, *24*). While mass spectrometry confirmed the existence of sulfated, hybrid oligosaccharides, they were not the most abundant species. Instead, the most abundant oligosaccharides were small, high-mannose types, possessing 3−6 mannose residues (structures 3, 6, and 10). Carbohydrate recoveries from preparative oligosaccharide mapping experiments provided additional support for this conclusion. The oligosaccharide mixture composition in previous studies was misleading because two

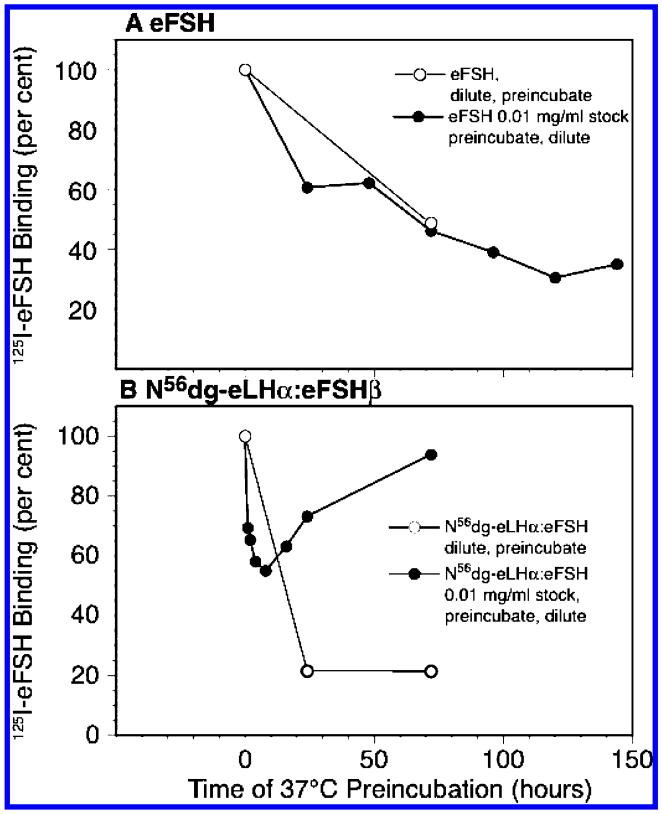

FIGURE 10: Stability of eFSH and N[56]-deglycosylated eFSH. Hormone samples were incubated at 37 °C for the indicated times, and competition curves were determined as described under the Materials and Methods. Relative potencies indicated the extent of subunit dissociation. Open symbols indicate previously reported data (*22*). Closed symbols indicate data derived from the present study.

other oligosaccharide classes, biantennary sulfated and hybrid sulfated, were present in sufficient abundance to yield an overall monosaccharide composition resembling that of a hybrid oligosaccharide (*10*). The larger oligosaccharides also contributed to an average Asn[56] carbohydrate mass of 1482, which was higher than that of structure 10, the largest and apparently most abundant high-mannose oligosaccharide (*m*/*z* 1257.4 for the sodium adduct). Nevertheless, the absence of a complex oligosaccharide branch, linking *β*(1−4) to the α-(1−6)Man of the pentasaccharide core, was confirmed for the vast majority of eLHα Asn[56] oligosaccharides. One minor population was completely overlooked in the MS of mixed oligosaccharides. Although monosaccharide composition had indicated 10% of eLHα Asn[56] oligosaccharides possessed fucose (*10*, *28*), no fucosylated oligosaccharides were detectable during MALDI−MS analysis of the oligosaccharide mixtures. These species appeared when partially purified eLHα oligosaccharide fractions were characterized.

Three biantennary, eFSHα oligosaccharides, one terminated with two sulfates, one terminated with two sialic acids, and one terminated with sulfate on one branch and sialic acid on the other, were consistent with previously reported composition data (*10*, *11*). However, oligosaccharide mapping and an average carbohydrate mass of 1883, suggested the presence of smaller, uncharacterized species. The sulfated/sialylated oligosaccharide (structure 61) was observed during MS in both positive- and negative-ion modes. The disulfated oligosaccharide (structure 52) was also encountered; however, the disialylated structure was not among the major eFSHα oligosaccharides. Smaller oligosaccharides, which were also fairly abundant, for the most part, appeared to be incompletely processed precursors of the major biantennary structures. However, an additional abundant class of high-mannose oligosaccharides was encountered, including phosphorylated high-mannose oligosaccharides (for example, structure 14). The latter may be significant, because it could provide a link to other signaling pathways, thereby providing a mechanism for the high biological activity associated with eFSH preparations as compared with porcine, ovine, and human FSH preparations (*22*, *29*, *30*). While fucosylated oligosaccharides comprised only 20% of the eFSHα oligosaccharide mixture, they were readily detected by MS. Thus, the detection limit for a particular oligosaccharide class in complex carbohydrate mixtures lies somewhere between 10 and 20% and is undoubtedly affected by heterogeneity of the population representing that class.

We previously concluded the two major eCGα Asn[56] oligosaccharide fractions consisted of biantennary oligosaccharides, both terminated with two sialic acid residues, with one branch extended by a lactosamine repeat (*10*, *11*). The most abundant oligosaccharides encountered in the present study were variants of the smaller biantennary oligosaccharide structure terminated with either Neu5Ac or another sialic acid derivative, possibly Neu5Gc. An O-acetylated sialic acid derivative, Neu4,5Ac$_2$, was reported in 20% of the biantennary oligosaccharides recovered from both eCGα N-glycosylation sites and on triantennary oligosaccharides attached to eCG*β* Asn[13] (*31*). This modification would have increased the oligosaccharide mass by 42 rather than the observed increase of 16. Oligosaccharides possessing the unidentified constituent did not appear in the negative ion spectrum nor did the sodium salt form appear in the positive ion spectrum. However, an unknown structural feature contributed to the small difference in retention time between the two most abundant eCGα Asn[56] oligosaccharide fractions (designated peaks 17 and 18) observed during oligosaccharide mapping experiments (*10*). We reported that peak 18 shared the same retention time as a reference biantennary oligosaccharide terminated with two Neu5Ac residues and suggested that peak 17 retention time was reduced by the presence of a lactosamine repeat (*10*, *32*). Because Neu5Gc oligosaccharides exhibited longer retention times than corresponding oligosaccharides possessing Neu5Ac (*32*), the shorter retention time for peak 17 supported our conclusion that the sialic acid derivative was not Neu5Gc. Although numerous but very low abundance ions corresponding to oligosaccharide structures possessing a lactosamine repeat were encountered during MS, notably structures 72, 74, and 79−90, their low abundance and structural heterogeneity argued against carbohydrate possessing lactosamine repeats comprising major peak 18. Low abundance could be a reflection of either the structural hetereogeneity or the acid labile nature of the lactosamine structure. While identifying O-glycosylation sites, mild acid hydrolysis not only quantitatively removed sialic acid from eCG*β*, but also removed GlcNAc and Gal, when the breakthrough fraction of the reverse-phase HPLC chromatogram was analyzed (*12*). Much of this acid-labile carbohydrate was probably derived from the O-linked oligosaccharides attached to a dozen O-glycosylation sites in the C terminus, which are also known to possess lactosamine repeats (*12*, *33*), but some could have been

derived from N-linked oligosaccharides. More likely, low lactosamine-possessing oligosaccharide abundance in this study stemmed from the high degree of structural heterogeneity.

While reduced receptor-binding affinity on the part of the eFSHα:eLHβ and eCGα:eLHβ hybrids appeared to be due to steric hindrance, elimination of the lactosamine-extended Man(α1−6)Man oligosaccharide branch as a major component of the eCGα Asn^{56} oligosaccharides made this carbohydrate population more similar to the expected sulfate/sialic-acid-terminated biantennary eFSHα Asn^{56} oligosaccharides. These oligosaccharides should have provided the same degree of steric hindrance as exclusively sialylated eCGα Asn^{56} oligosaccharides, especially because the exchange of sulfate-terminated oligosaccharides for sialic-acid-terminated oligosaccharides did not appear to affect bLH biological activity (*34*). The presence of abundant, smaller oligosaccharides in the eFSHα oligosaccharide mixture, provided a rationale for the greater receptor-binding affinity for eFSHα:eLHβ as compared with eCGα:eLHβ, especially because α-subunit preparations possessing smaller oligosaccharides combined with eLHβ to a greater extent than those with larger oligosaccharides (*11*). Moreover, analysis of unassociated α-subunit fraction Asn^{56} oligosaccharides revealed that those in eCGα:eLHβ were virtually all biantennary, while those in eFSHα:eLHβ were enriched for smaller oligosaccharides (*11*). Thus, we returned to our earlier hypothesis that the presence of a complex oligosaccharide branch, attached β-(1−4) to the (α1−6)Man of the pentasaccharide core, inhibited LH receptor-binding, perhaps explaining the general absence of this branch from LH and hCG αL2 oligosaccharides.

The equine pituitary gonadotropins, eLH and eFSH, provide interesting contrasts in stability. At nanogram per milliliter concentrations, 50% of eFSH dissociated into subunits following incubation for 72 h at 37 °C, while eLH remained intact (*22*). Intact eLH was stable at pH 7.4 and 3, for at least 72 h at 25 °C, while 95% of intact eFSH dissociated into subunits after 20−30 min at pH 3 (*16*). Both intact eLH and Asn^{56}-dg-eLH hybrid preparations were stable at pH 7.4 and 37 °C for at least 72 h (*22*). While the intact eFSH hybrid preparations exhibited no significant differences in either FSH receptor-binding activity or CD spectrum, following removal of αAsn^{56} oligosaccharide, the CD spectra displayed increased negative ellipticity at 210 nm for N^{56}dg-eLHα:eFSHβ and to a lesser extent for N^{56}dg-eFSHα:eFSHβ. Both preparations displayed increased α-helical content, while a reduction in β-sheet content was noted only for N^{56}dg-eLHα:eFSHβ. Receptor-binding activities for both preparations were reduced as compared with their intact counterparts, instead of the increased activity normally associated with elimination of this oligosaccharide from LH and CG preparations. A small reduction in negative ellipticity was noted for N^{56}dg-eCGα:eFSHβ, along with little change in the secondary structure. Interestingly, the latter did not lose FSH receptor-binding activity, while the other two hybrids lost 21−29% receptor-binding activity. Stability studies suggested that 35% subunit dissociation of N^{56}dg-eLHα:eFSHβ occurred during the incubation period for 2 h employed in the radioligand assay, similar to the 29% reduction in FSH receptor-binding activity. Although the N^{56}dg-eCGα:eFSHβ preparation appeared to exhibit greater stability than the other N^{56}dg-α:eFSHβ hybrid preparations, suggesting a potential stabilizing role for eCGαAsn^{82} oligosaccharide, follow-up studies were prevented by a lack of material.

The existence of stable FSH isoforms indicated by the rapid dissociation of N^{56}dg-eFSHα:eFSHβ followed by the slow reassociation of a more stable form is not unprecedented. Intact hFSH preparations possessed 52−57% nondissociable heterodimer (*35*, *36*). Significant amounts (33−50%) of nondissociable bFSH have been reported (*37*, *38*). We have encountered nondissociable eFSH during subunit isolation. However, because it overlaped with the subunit fraction, estimation of the relative proportion of the stable eFSH isoform has not been possible. Ovine LH preparations possess 10% nondissociable hormone that cannot be separated by a variety of denaturing conditions including 6−8 M GuHCl dissociation or 2% SDS and 5% 2-mercaptoethanol and boiling (*39*, *40*). Nondissociable oLH was largely inactive, while nondissociable eFSH retained receptor-binding activity. The functional but more stable eFSH isoform will be interesting to study in the future.

ACKNOWLEDGMENT

The technical assistance of Vanda Baker and Wendy Walton in preparative oligosaccharide isolation is gratefully acknowledged. The TofSpec MALDI mass spectrometer was provided by funds from the Biotechnology Sciences Research Council. We thank Waters-Micromass for access to the MALDI-Q-TOF mass spectrometer.

SUPPORTING INFORMATION AVAILABLE

This material is available free of charge via the Internet at http://pubs.acs.org.

REFERENCES

1. Hearn, M. T. W., and Gomme, P. T. (2000) Molecular architecture and biorecognition processes of the cystine knot protein superfamily: Part I. The glycoprotein hormones, *J. Mol. Recognit. 13*, 223−278.
2. Aloj, S. M., Edelhoch, H., Ingram, K. C., Morgan, F. J., Canfield, R. E., and Ross, G. T. (1973) The rates of dissociation and reassociation of the subunits of human chorionic gonadotropin, *Arch. Biochem. Biophys. 159*, 497−504.
3. Reichert, L. E., Jr., Trowbridge, C. G., Bhalla, V. K., and Lawson, G. M. (1974) The kinetics of formation and biological activity of native and hybrid molecules of human follicle-stimulating hormone, *J. Biol. Chem. 249*, 6472−6477.
4. Xie, Y.-B., Wang, H., and Segaloff, D. L. (1990) Extracellular domain of lutropin/choriogonadotropin receptor expressed in transfected cells binds choriogonadotropin with high affinity, *J. Biol. Chem. 35*, 21411−21414.
5. Ji, T. H., and Ji, I. (1993) Receptor activation is distinct from hormone binding in intact lutropin-choriogonadotropin receptors and Asp397 is important for receptor activation, *J. Biol. Chem. 268*, 20851−20854.
6. Matzuk, M. M., Keene, J. L., and Boime, I. (1989) Site specificity of the chorionic gonadotropin N-linked oligosaccharides in signal transduction, *J. Biol. Chem. 264*, 2409−2414.
7. Bishop, L. A., Robertson, D. M., Cahir, N., and Schofield, P. R. (1994) Specific roles for the asparagine-linked carbohydrate residues of recombinant human follicle stimulating hormone in receptor binding and signal transduction, *J. Mol. Endocrinol. 8*, 722−731.
8. Flack, M. R., Froehlich, J., Bennet, A. P., Anasti, J., and Nisula, B. C. (1994) Site-directed mutagenesis defines the individual roles of the glycosylation sites on follicle-stimulating hormone, *J. Biol. Chem. 269*, 14015−14020.

9. Liu, W. K., Young, J. D., and Ward, D. N. (1984) Deglycosylated ovine lutropin: Preparation and characterization by in vitro binding and steroidogenesis, *Mol. Cell. Endocrinol. 37*, 29−39.
10. Gotschall, R. R., and Bousfield, G. R. (1996) Oligosaccharide mapping reveals hormone-specific glycosylation patterns on equine gonadotropin α-subunit Asn[56], *Endocrinology 137*, 2543−2557.
11. Butnev, V. Y., Gotschall, R. R., Butnev, V. Y., Baker, V. L., Moore, W. T., and Bousfield, G. R. (1998) Hormone-specific inhibitory influence of α-subunit Asn[56] oligosaccharide on *in vitro* subunit association and FSH receptor binding of equine gonadotropins, *Biol. Reprod. 58*, 458−469.
12. Bousfield, G. R., Butnev, V. Y., and Butnev, V. Y. (2001) Identification of twelve-O-glycosylation sites in eCGβ and eLHβ by solid-phase Edman degradation, *Biol. Reprod. 64*, 136−147.
13. Bousfield, G. R., and Ward, D. N. (1984) Purification of lutropin and follitropin in high yield from horse pituitary glands, *J. Biol. Chem. 259*, 1911−1921.
14. Butnev, V. Y., Gotschall, R. R., Baker, V. L., Moore, W. T., and Bousfield, G. R. (1996) Negative influence of O-linked oligosaccharides of high molecular weight equine chorionic gonadotropin on its luteinizing hormone and follicle-stimulating hormone receptor-binding activities, *Endocrinology 137*, 2530−2542.
15. Bousfield, G. R., Liu, W.-K., and Ward, D. N. (1985) Hybrids from equine LH: α enhances, β diminishes activity, *Mol. Cell. Endocrinol. 40*, 69−77.
16. Bousfield, G. R., and Ward, D. N. (1986) Direct demonstration of intrinsic follicle-stimulating hormone receptor-binding activity in acid-treated equine luteinizing hormone, *Biochim. Biophys. Acta 885*, 327−334.
17. Packer, N. H., Lawson, M. A., Jardine, D. R., and Redmond, J. W. (1998) A general approach to desalting oligosaccharides released from glycoproteins, *Glycoconjugate J. 15*, 737−747.
18. Bousfield, G. R., Baker, V. L., Gotschall, R. R., Butnev, V. Y., and Butnev, V. Y. (2000) Carbohydrate analysis of glycoprotein hormones, *Methods 21*, 15−39.
19. Börnsen, K. O., Mohr, M. D., and Widmer, H. M. (1995) Ion exchange and purification of carbohydrates on a Nafio membrane as a new sample pretreatment for matrix-assisted laser-desorption-ionization mass spectrometry, *Rapid Commun. Mass Spectrom. 9*, 1031−1034.
20. Mattu, T. S., Royle, L., Langridge, J., Wormald, M. R., van den Steen, P. E., Van Damme, J., Opdenakker, G., Harvey, D. J., Dwek, R. A., and Rudd, P. M. (2000) O-glycan analysis of natural human neutrophil gelatinase B using a combination of normal phase-HPLC and online tandem mass spectrometry: Implications for the domain organization of the enzyme, *Biochemistry 39*, 15695−15704.
21. Sreerama, N., and Woody, R. W. (2000) Estimation of protein secondary structure from circular dichroism spectra: Comparison of CONTIN, SELCON, and CDSSTR methods with an expanded reference set, *Anal. Biochem. 287*, 252−260.
22. Butnev, V. Y., Singh, V., Nguyen, V. T., and Bousfield, G. R. (2002) Truncated eLHβ and asparagine[56]-deglycosylated eLHα combine to produce a potent follicle-stimulating hormone antagonist, *J. Endocrinol. 172*, 545−555.
23. Weisshaar, G., Hiyama, J., and Renwick, A. G. C. (1990) Site-specific N-glycosylation of ovine lutropin: Structural analysis by one- and two-dimensional ^{1}H NMR spectroscopy, *Eur. J. Biochem. 192*, 741−751.
24. Weisshaar, G., Hiyama, J., and Renwick, A. G. C. (1991) Site-specific N-glycosylation of human chorionic gonadotropin—Structural analysis of glycopeptides by one- and two-dimensional ^{1}H NMR spectroscopy, *Glycobiology 1*, 393−404.
25. Lapthorn, A. J., Harris, D. C., Littlejohn, A., Lustbader, J. W., Canfield, R. E., Machin, K. J., Morgan, F. J., and Isaacs, N. W. (1994) Crystal structure of human chorionic gonadotropin, *Nature 369*, 455−461.
26. Wu, H., Lustbader, J. W., Liu, Y., Canfield, R. E., and Hendrickson, W. A. (1994) Structure of human chorionic gonadotropin at 2.6 Å resolution from MAD analysis of the selenomethionyl protein, *Structure 2*, 545−558.
27. Fox, K. M., Dias, J. A., and Van Roey, P. (2001) Three-dimensional structure of human follicle-stimulating hormone, *Mol. Endocrinol. 15*, 378−389.
28. Nguyen, V. T., Singh, V., Butnev, V. Y., Gray, C. M., Westfall, S., Davis, J. S., Dias, J. A., and Bousfield, G. R. (2003) Inositol phosphate stimulation by LH requires the entire α Asn[56] oligosaccharide, *Mol. Cell. Endocrinol. 199*, 73−86.
29. Combarnous, Y., Guillou, F., and Martinat, N. (1984) Comparison of *in vitro* follicle-stimulating hormone (FSH) activity of equine gonadotropins (luteinizing hormone, FSH, and chorionic gonadotropin) in male and female rats, *Endocrinology 115*, 1821−1827.
30. Liu, W.-K., Bousfield, G. R., Moore, W. T., Jr., and Ward, D. N. (1985) Priming procedure and hormone preparations influence rat granulosa cell response, *Endocrinology 116*, 1454−1459.
31. Damm, J. B. L., Hard, K., Kammerling, J. P., van Dedem, G. W. K., and Vliegenthart, F. G. (1990) Structure determination of the major N- and O-linked carbohydrate chains of the β subunit from equine chorionic gonadotropin, *Eur. J. Biochem. 189*, 175−183.
32. Hermentin, P., Witzel, R., Vliegenthart, J. F. G., Kamerling, J. P., Nimtz, M., and Conradt, H. S. (1992) A strategy for the mapping of N-glycans by high-pH anion-exchange chromatography with pulsed amperometric detection, *Anal. Biochem. 203*, 281−289.
33. Hokke, C. H., Roosenboom, M. J. H., Thomas-Oates, J. E., Kamerling, J. P., and Vliegenthart, J. F. G. (1994) Structure determination of the disialylated poly-(*N*-acetyllactosamine)-containing O-linked carbohydrate chains of equine chorionic gonadotropin, *Glycoconjugate J. 11*, 35−41.
34. Baenziger, J. U., Kumar, S., Brodbeck, R. M., Smith, P. L., and Beranek, M. C. (1992) Circulatory half-life but not interaction with the lutropin/chorionic gonadotropin receptor is modulated by sulfation of bovine lutropin oligosaccharides, *Proc. Natl. Acad. Sci. U.S.A. 89*, 334−338.
35. Rathnam, P., and Saxena, B. B. (1975) Primary amino acid sequence of follicle-stimulating hormone from human pituitary glands I. α subunit, *J. Biol. Chem. 250*, 6735−6746.
36. Parlow, A. F., and Shome, B. (1974) Specific, homologous radioimmunoassay (RIA) of highly purified subunits of human pituitary follicle stimulating hormone (hFSH), *J. Clin. Endocrinol. Metab. 39*, 195−198.
37. Grimek, H. J., Gorski, J., and Wentworth, B. C. (1979) Purification and characterization of bovine follicle-stimulating hormone: Comparison with ovine follicle-stimulating hormone, *Endocrinology 104*, 140−147.
38. Cheng, K. W. (1977) Presence of subunit structure in bovine follicle-stimulating hormone, *Endocr. Res. Commun. 4*, 25−34.
39. Liu, W.-K., Ascoli, M., and Ward, D. N. (1977) Ovine lutropin subunit isolation: Comparison of salt precipitation and countercurrent distribution procedures, *J. Biol. Chem. 252*, 5274−5279.
40. Bousfield, G. R., and Ward, D. N. (1994) Evidence for two folding domains in glycoprotein hormone α subunits, *Endocrinology 135*, 624−635.
41. Harvey, D. J., Hunter, A. P., Bateman, R. H., Brown, J., and Critchley, G. (1999) Relationship between in-source and post-source fragment ions in the matrix-assisted laser desorption (ionization) mass spectra of carbohydrates recorded with reflectron time-of-flight mass spectrometers, *Int. J. Mass Spectrom. 188*, 131−146.

BI049857P